# MESSENGER: Exploring Mercury's Magnetosphere

James A. Slavin[1], Stamatios M. Krimigis[2], Mario H. Acuña[1], Brian J. Anderson[2], Daniel N. Baker[3], Patrick L. Koehn[4], Haje Korth[2], Stefano Livi[2], Barry H. Mauk[2], Sean C. Solomon[5], and Thomas H. Zurbuchen[4]

[1]Laboratory for Solar and Space Physics, Goddard Space Flight Center, Greenbelt, MD 20771

[2] Johns Hopkins Laboratory, Applied Physics Laboratory, Laurel, MD 20723

[3] Laboratory for Atmospheric and Space Physics, University of Colorado, Boulder, CO 80303

[4] Oceanic and Space Sciences Department, University of Michigan, Atmospheric, Ann Arbor, MI 48109

[5] Department of Terrestrial Magnetism, Carnegie Institution of Washington, Washington, DC 20015

Submitted to *Space Science Reviews*, 2005

Dec 19, 2005 Draft

**Abstract.** The MESSENGER mission to Mercury offers our first opportunity to explore this planet's miniature magnetosphere since the brief flybys of Mariner 10. Mercury's magnetosphere is unique in many respects. The magnetosphere of Mercury is among the smallest in the solar system; its magnetic field typically stands off the solar wind only ~ 1000 to 2000 km above the surface. For this reason there are no closed drift paths for energetic particles and, hence, no radiation belts. The characteristic time scales for wave propagation and convective transport are short and kinetic and fluid modes may be coupled. Magnetic reconnection at the dayside magnetopause may erode the subsolar magnetosphere allowing solar wind ions to impact directly the regolith. Inductive currents in Mercury's interior may act to modify the solar wind interaction by resisting changes due to solar wind pressure variations. Indeed, observations of these induction effects may be an important source of information on the state of Mercury's interior. In addition, Mercury's magnetosphere is the only one with its defining magnetic flux tubes rooted in a planetary regolith as opposed to an atmosphere with a conductive ionospheric layer. This lack of an ionosphere is probably the underlying reason for the brevity of the very intense, but short-lived, ~ 1-2 min, substorm-like energetic particle events observed by Mariner 10 during its first traversal of Mercury's magnetic tail. Because of Mercury's proximity to the sun, 0.3 – 0.5 AU, this magnetosphere experiences the most extreme driving forces in the solar system. All of these factors are expected to produce complicated interactions involving the exchange and re-cycling of neutrals and ions between the solar wind, magnetosphere, and regolith. The electrodynamics of Mercury's magnetosphere are expected to be equally complex, with strong forcing by the solar wind, magnetic reconnection at the magnetopause and in the tail, and the pick-up of planetary ions all driving field-aligned electric currents. However, these field-aligned currents do not close in an ionosphere, but in some other manner. In addition to the insights into magnetospheric physics offered by study of the solar wind - Mercury system, quantitative specification of the "external" magnetic field generated by magnetospheric currents is necessary for accurate determination of the strength and multi-polar decomposition of Mercury's intrinsic magnetic field. MESSENGER's highly capable instrumentation and broad orbital coverage will greatly advance our understanding of both the origin of Mercury's magnetic field and the acceleration of charged particles in small magnetospheres. In this article, we review what is known about Mercury's magnetosphere and describe the MESSENGER science team's strategy for obtaining answers to the outstanding science questions surrounding the interaction of the solar wind with Mercury and its small, but dynamic, magnetosphere.

## 1. Introduction: What do we presently know and how do we know it?

Launched on November 2, 1973, Mariner 10 (M10) executed the first reconnaissance of Mercury during its three encounters on March 29, 1974, September 21, 1974, and March 16, 1975 (see reviews by Russell *et al.*, 1988; Slavin, 2004; Milillo et al., 2005). All fly-bys occurred at a heliocentric distance of 0.46 AU, but only the first (Mercury I) and third (Mercury III) encounters passed close enough to Mercury to return observations of the solar wind interaction and the planetary magnetic field. The first encounter targeted the planetary "wake" and returned surprising observations that indicate a significant intrinsic magnetic field. The closest approach to the surface during this passage was 723 km where a peak magnetic field intensity of 98 nT was observed (Ness *et al.*, 1974). During Mercury I the magnetic field investigation observed clear bow shock and magnetopause boundaries along with the lobes of the tail and the cross-tail current layer (Ness *et al.*, 1974; 1975; 1976). The Mercury III observations were of great importance because they confirmed that the magnetosphere was indeed produced by the interaction of the solar wind with an intrinsic planetary magnetic field. Once corrected for the differing closest approach distances, the polar magnetic fields measured during Mercury III are about twice as large as those along the low latitude Mercury I trajectory, consistent with a primarily dipolar planetary field.

The plasma investigation was hampered by a deployment failure that kept it from returning ion measurements. Fortunately, the electron portion of the plasma instrument did operate as planned (Ogilvie *et al.*, 1974). Good correspondence was found between the magnetic field and plasma measurements as to the locations of the Mercury I and III bow shock and magnetopause boundaries. Plasma speed and density parameters derived from the electron data produced consistent results regarding bow shock jump conditions and pressure balance across the magnetopause (Ogilvie *et al.*, 1977; Slavin *et al.*, 1979a). Within Mercury's magnetosphere, plasma density was found to be higher than that observed at Earth by a factor comparable to the ratio of the solar wind density at the orbits of the two planets (Ogilvie *et al.*, 1977). Similar correlations are observed between solar wind and plasma sheet density at Earth (Teresawa *et al.*, 1997). Throughout the Mercury I pass plasma sheet-type electron distributions were observed with an increase in temperature beginning near closest approach coincident with several intense energetic particle events (Ogilvie *et al.*, 1977; Christon, 1987).

Several groups have estimated the magnetic moment of Mercury from the observations made during Mercury I and III. Conducting a least-squared fit of the Mercury I data to an offset tilted dipole, Ness *et al.* (1974) obtained a dipole moment of 227 nT$R_M^3$, where $R_M$ is Mercury's radius (1 $R_M$ = 2439 km), and a dipole tilt angle of 10 deg relative to the planetary rotation axis. Ness *et al.* (1975) considered a centered dipole and an external contribution to the measured magnetic field and found the strength of the dipole to be 349 nT$R_M^3$ from the same data set. From the Mercury III encounter observations these authors determined a dipole moment of 342 nT$R_M^3$. (Ness *et al.*, 1976). Higher-order contributions to the internal magnetic field were examined by Jackson and Beard (1977) (quadrupole) and Whang (1977) (quadrupole, octupole). Both sets of authors reported

170 nT$R_M^3$ as the dipole contribution to Mercury's intrinsic magnetic field. The cause for the large spread in the reported estimates of the dipole term is the limited spatial coverage of the observations, which is insufficient for separating the contributions from higher-order multipoles (Connerney and Ness, 1988) and magnetic fields due to magnetospheric current systems (Slavin and Holzer, 1979b; Korth *et al.*, 2004).

Mercury's magnetosphere is one of the most dynamic in the solar system. A glimpse of this variability was captured during the Mercury I encounter. Less than a minute after M10 entered the plasma sheet during this first flyby there was a sharp increase in the $B_z$ field component (Ness *et al.*, 1974). The initial sudden $B_z$ increase and subsequent quasi-periodic increases are nearly coincident with strong enhancements in the flux of >35 keV electrons observed by the cosmic ray telescopes (Simpson *et al.,* 1974; Eraker and Simpson, 1986; Christon, 1987). Taken together, these M10 measurements are very similar to the "dipolarizations" of the near-tail magnetic field frequently observed in association with energetic particle "injections" at Earth (Christon *et al.*, 1987). This energetic particle signature, and several weaker events observed later in the outbound Mercury I pass, was interpreted as strong evidence for substorm activity and, by inference, magnetic reconnection in the tail (Siscoe *et al.*, 1975; Eraker and Simpson, 1986; Baker *et al.,* 1986; Christon, 1987).

The stresses exerted on planetary magnetic fields by magnetospheric convection are transmitted down to the planet and its environs by field-aligned currents. At planets with electrically conductive ionospheres, such as the Earth, Jupiter and Saturn, these current systems are well observed and constitute an important energy sink for these magnetospheres as well as serving as a "brake" that limits the speed and rate of change of the plasma convection (Coroniti and Kennel, 1973). Mercury's atmosphere, however, is a tenuous exosphere, and no ionosphere possessing significant electrical conductance is present (Lanner and Bauer, 1997). For these reasons, the strong variations in the east-west component of the magnetic field measured by M10 during the Mercury I pass several minutes following the substorm-like signatures may be quite significant. These perturbations were first examined by Slavin *et al.* (1997) who concluded that the spacecraft crossed three field-aligned current (FAC) sheets similar to those often observed at the Earth (Iijima and Potemra, 1978). The path by which these currents close is not known, but their existence may indicate that the conductivity of the regolith is greater than is usually assumed on the basis of analogy with the lunar surface (e.g., Hill *et al.*, 1976). Indeed, arguments can be made for a wide range of regolith conductivities (Glassmeier, 1997; Janhunen and Kallio, 2004). In addition, the process by which newly created heavy ions are "picked up" by Mercury's magnetosphere creates an electrical current which may contribute to FAC closure. Cheng *et al.* (1987) estimated that the magnitude of such a "pickup conductance" at Mercury could reach ~0.3 mho, but this number is highly uncertain. Finally, Glassmeier (1997) showed that the Alfven conductance associated with magnetohydrodynamic (MHD) wave propagation could reach ~ 1 mho depending upon the heavy ion densities.

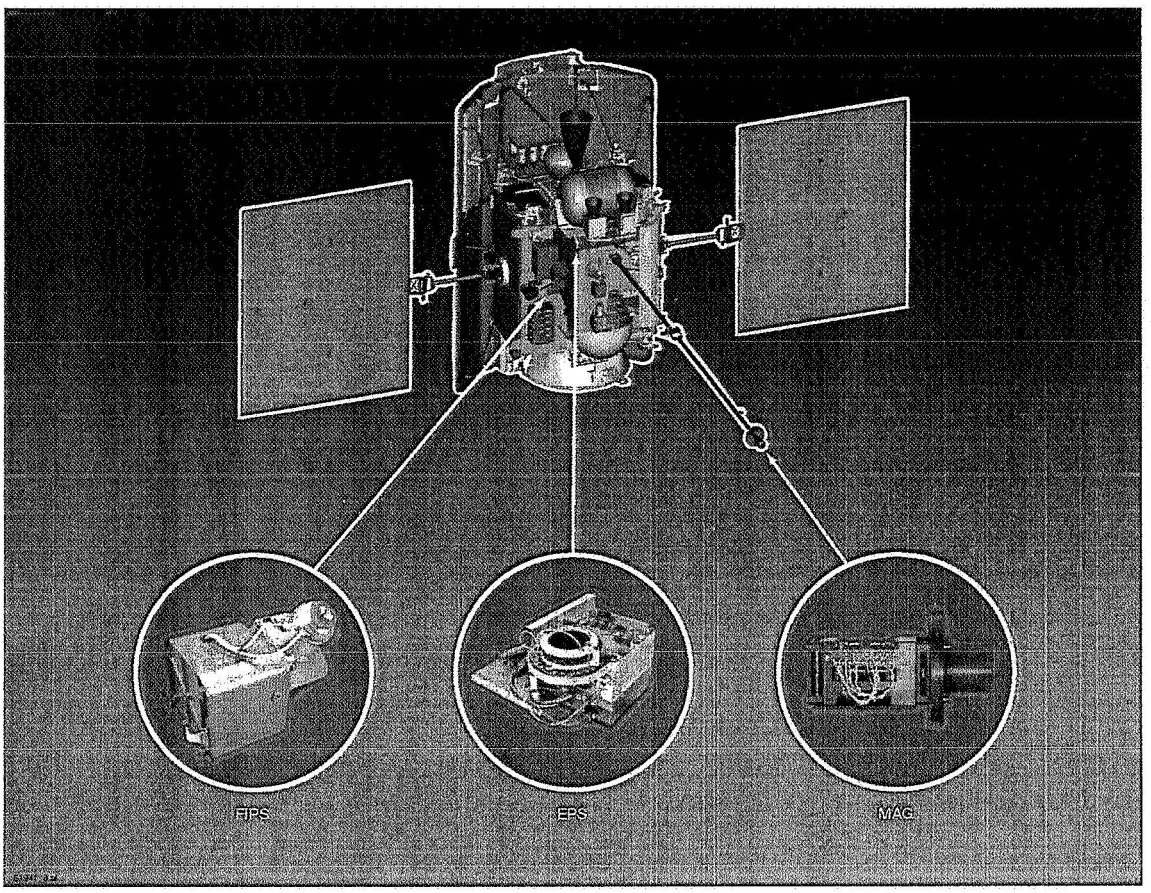


Figure 1. The MESSENGER spacecraft behind its sunshade. Note the adapter ring at the bottom of the vehicle which encloses the planet nadir pointing instruments. The Magnetometer (MAG) is located at the end of a 3.6 m double-hinged boom along with its own small "dog-collar" sunshade. The FIPS and EPS sensors (blue) are shown along with arrows indicating their location on the spacecraft.

Another unique aspect of Mercury concerns the origin of its very tenuous, collisionless, neutral atmosphere (e.g., Goldstein et al., 1981). Three exospheric neutral species, Na, K, and Ca, have been measured spectroscopically from the Earth (Potter and Morgan, 1985; 1986; Bida *et al.*, 2000). The large day-to-day variability in the sodium and potassium exosphere at Mercury, including changes in both total density and global distribution, are quite striking and may be linked to dynamic events in the solar wind and their effect on the magnetosphere. For example, Potter *et al.* (1999) suggested that the underlying cause of the large day-to-day changes in the neutral exosphere might be the modulation of the surface sputtering rates by variations in the spatial distribution and intensity of solar wind proton impingement on the surface. Our present understanding of Mercury's neutral atmosphere and the contributions that MESSENGER will make to this discipline are the subject of a companion paper by Domingue *et al.* (2005).

## 2. MESSENGER Science Instruments

The MESSENGER spacecraft, instrument payload, and mission plan have been described elsewhere (Gold *et al.*, 2001). Here we provide a brief overview to emphasize the nature of the measurements to be

returned and how they will be used to achieve the mission's scientific objectives (Solomon *et al.*, 2001). The MESSENGER spacecraft is shown in Figure 1. The key aspect of its design is the presence of a large sunshade that will always face the sun once the spacecraft is closer than 0.9 AU to the sun. The spacecraft is three-axis stabilized, but rotations about the Sun – spacecraft axis will be carried out to orient some of the instruments toward the surface.

The MESSENGER Magnetometer (MAG) is described in detail by Anderson *et al.* (2005). The triaxial sensor is mounted at the end of a 3.6-m boom to minimize the magnitude of stray spacecraft-generated magnetic fields at the MAG sensor location. Ground testing and in-flight calibration have shown that the intensity of uncorrectable (i.e., variable) stray fields will be less than 0.1 nT (Anderson *et al.*, 2005). While the magnetometer is capable of measuring the full strength of the Earth's field for integration and check-out reasons, it is designed to operate in its most sensitive field range of +/- 1500 nT per axis when the spacecraft is orbit about Mercury. The 16-bit telemetered resolution yields a digital resolution of 0.05 nT. In the baseline mission plan, the sampling rate of the instrument will be varied according to a pre-planned schedule from 2 to 20 vectors $s^{-1}$ once in orbit about Mercury. Additionally, 8-minute intervals of 20-vectors $s^{-1}$ burst data will be acquired during periods of lower-rate continuous sampling. The accuracy of the MESSENGER magnetic field measurements is 0.1%.

The MESSENGER Energetic Particle and Plasma Spectrometer (EPPS) instrument is described in detail by Andrews *et al.* (2005). EPPS is composed of two charged particle detector systems, the Fast Imaging Plasma Spectrometer (FIPS) and the Energetic Particle Spectrometer (EPS). FIPS has a near-hemispherical field of view and accepts ions with an energy-to-charge ratio from 0.05 to 20 keV/q. EPS has a $12^{\circ}$ x $160^{\circ}$ field of view and accepts ions and electrons with energies of 10 keV to 5 MeV and 10 keV to 400 keV, respectively. The EPPS sensors are mounted between the attach points for the MAG boom and one of the solar arrays. The field of views of both the FIPS and EPS are such that they will measure charged particles coming from the anti-sunward direction, as well as from above and below the spacecraft. The FIPS field of view also encompasses the sunward direction, but this portion of its field-of-view is blocked by the spacecraft and the sunshade. The EPPS measurements are central to resolving the issues that arose from the incomplete and ambiguous energetic particle measurements of M10. The energetic particle measurements of Simpson *et al.* (1974) were compromised by electron pileup in the proton channel (Armstrong *et al.*, 1975). They were later reinterpreted as having been responding to intense fluxes of > 35 keV electrons (Christon, 1987).

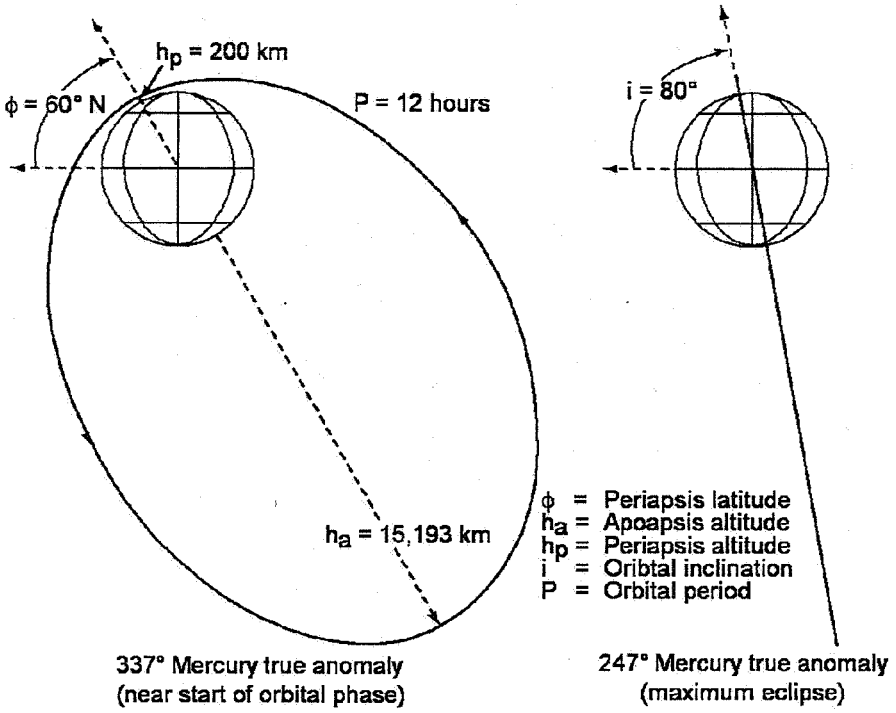


Figure 2. Orthogonal views of the 12-hr-long MESSENGER orbit. The left-hand image shows the orbital plane; periaspsis and apoapsis altitudes are 200 km and 15,193 km, respectively. The 80° inclination of the orbit is apparent in the orthogonal view in the right-hand image.

## 3. MESSENGER Mission Plan

When evaluating the potential scientific impact in-situ magnetospheric measurements, the spatial coverage of the various critical boundaries and regions is one of the most important factors. Figure 2 shows the highly inclined, eccentric orbit that MESSENGER will achieve following insertion and trim maneuvers. This orbit represents a carefully considered trade between the sometimes competing requirements of the planetary interior, surface geology, atmospheric and magnetospheric science investigations and engineering constraints, particularly those related to the thermal environment (Solomon *et al.*, 2001; Santo *et al.*, 2001). This orbit satisfies the primary requirements of all of these planetary science disciplines and will enable an outstanding set of measurements to be gathered.

From the standpoint of the magnetosphere, the most informative view of the MESSENGER orbital coverage is to examine it relative to the mean bow shock and magnetopause surfaces. These boundaries are, to first order, axially symmetric with respect to the X axis in Mercury-Solar-Orbital (MSO) coordinates. This coordinate system is the Mercury equivalent of the familiar Geocentric-Solar-Ecliptic (GSE) system used at the Earth. In this system $X_{MSO}$ is directed from the planet's center to the Sun, $Y_{MSO}$ is anti-parallel to the planetary velocity vector, and $Z_{MSO}$ completes the right handed system. For more detailed boundary modeling, the MSO

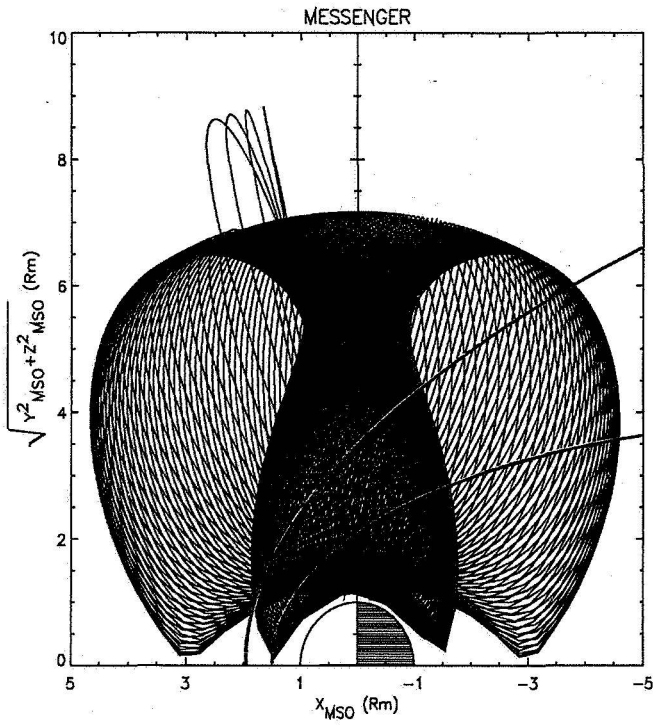


Figure 3a. Projection of the first Mercury year of predicted orbits for MESSENGER into the $X_{MSO} - (Y_{MSO}{}^2 + Z_{MSO}{}^2)^{1/2}$ plane. The conic traces in red are the expected mean locations of the magnetopause and bow shock boundaries on the basis of the two M10 encounters (Slavin and Holzer, 1979a).

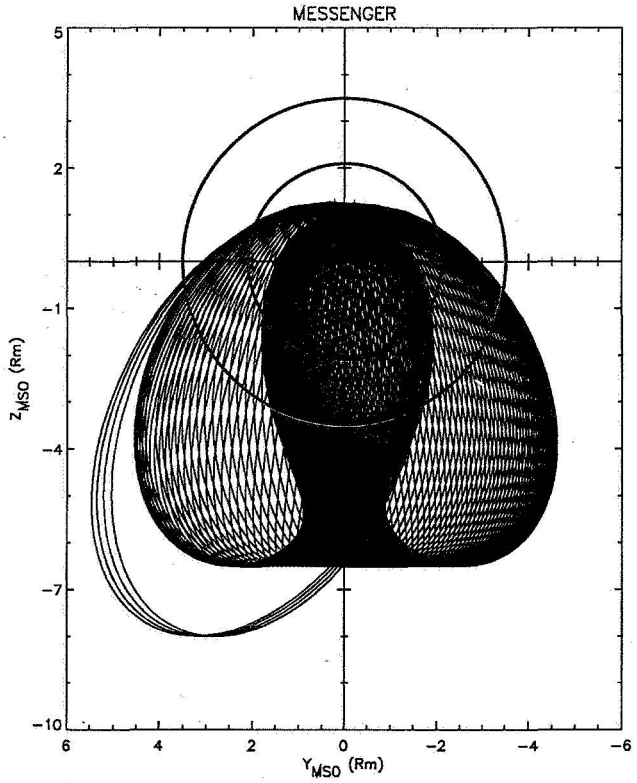


Figure 3b. Projection of the first Mercury year of predicted orbits for MESSENGER into the $Y_{MSO} - Z_{MSO}$ plane. The circular traces are the expected mean locations of the magnetopause and bow shock boundaries in the $X_{MSO} = 0$ plane on the basis of two M10 encounters (Slavin and Holzer, 1979a).

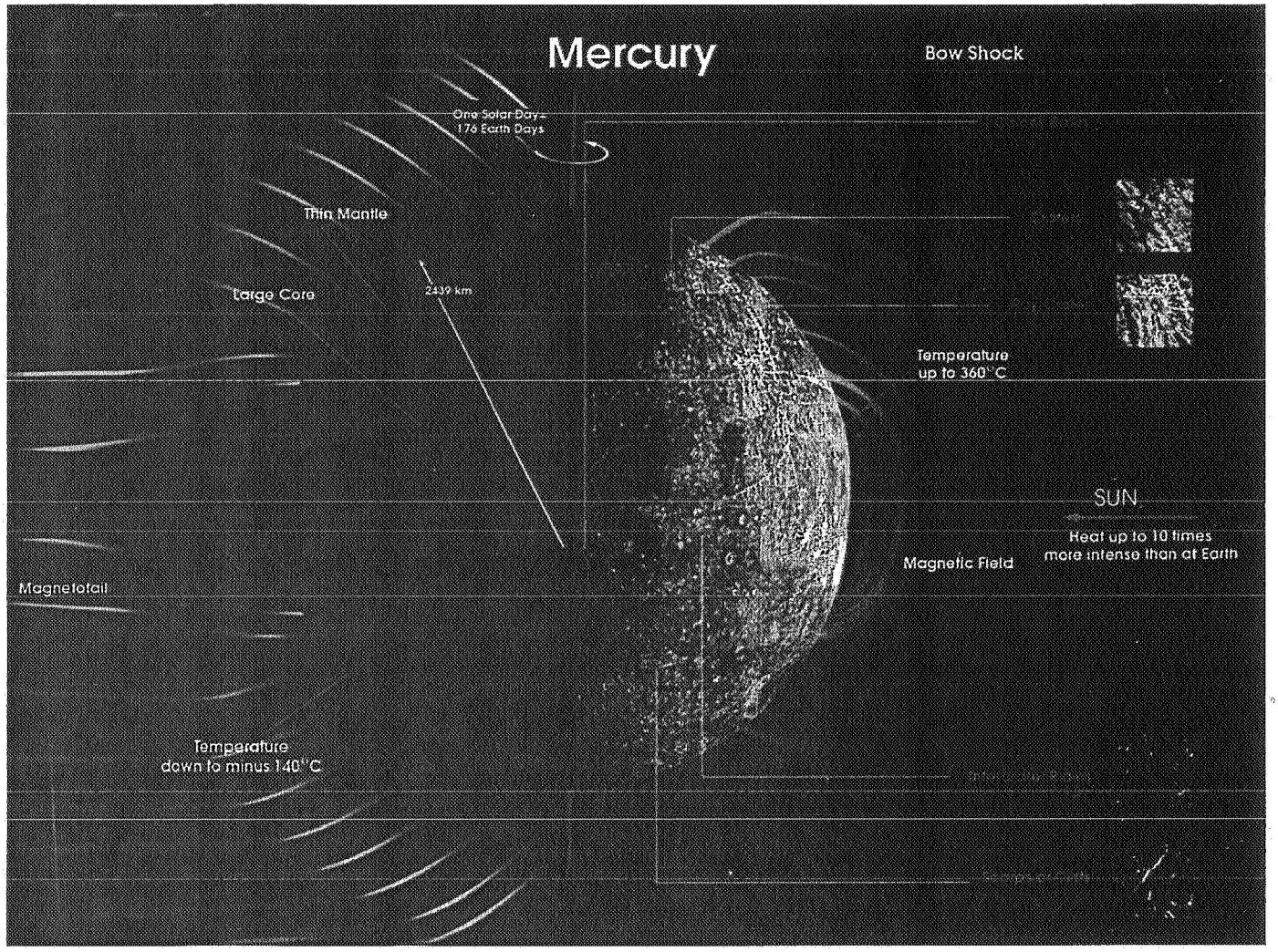


Figure 4. Mercury's magnetic field and the strong asymmetries introduced by its interaction with the solar wind (Copyright European Space Agency).

coordinates will be "aberrated" using the relative speeds of the planet and the solar wind so that the $X'_{MSO}$ axis is opposite to the mean solar wind velocity direction in the rest frame of Mercury (e.g., Slavin and Holzer, 1981).

The efficacy of the MESSENGER orbit for magnetospheric physics may be judged by plotting these boundaries and the trace of the orbit over a Mercury year in the $(Y_{MSO}^2 + Z_{MSO}^2)^{1/2}$ vs. $X_{MSO}$ and $Z_{MSO}$ vs. $Y_{MSO}$ planes. As displayed in Figures 3a and 3b, the bow shock and magnetopause boundaries in these planes appear as near-parabolic curves and concentric circles, respectively. The MESSENGER orbit will provide dense sampling of all of the primary regions of the magnetosphere and its interaction with the solar wind. The low-altitude polar passes in the northern hemisphere provide an excellent opportunity to observe and map field aligned currents. The region south of Mercury's orbital plane is better sampled at high altitudes than those to the north. However, we expect that Mercury's magnetosphere possesses considerable north-south symmetry. In this

manner, the MESSENGER orbit provides nearly comprehensive coverage of Mercury's magnetosphere and solar wind boundaries sunward of $X_{MSO} \sim -3\ R_M$.

## 4. Solar Wind – Magnetosphere Interaction

### 4.1 WHAT IS THE ORIGIN OF MERCURY'S MAGNETIC FIELD?

A planet's atmosphere, spin axis orientation and rotation rate, the existence and nature of any satellites and its location within the heliosphere are all important factors influencing magnetospheric structure and dynamics. However, the single most defining variable is the nature of its internal magnetic field. It consists of the magnetic field intrinsic to the planet and an external contribution due to magnetospheric currents. As shown in Figure 4, the sum of the primarily dipolar planetary magnetic field and the fields due to the external currents produce a magnetospheric magnetic field that is very different from a vacuum dipole even quite close to the planet's surface. On the dayside the magnetic field is greatly compressed; the intensity near the subsolar point is about twice that due to the planetary field alone. Conversely, the magnetic field on the nightside near midnight is somewhat reduced near the surface from that of the planetary field alone, but it is much stronger than the planetary dipole field at high altitudes where the flux tubes are pulled back to form the long extended magnetotail.

Possible sources for Mercury's magnetic field are an active dynamo, thermoremanent magnetization of the crust, or a combination thereof. On the basis of analogy with the Earth, it is often assumed that the source of Mercury's magnetic field is an active dynamo. Although thermal evolution models predict the solidification of a pure iron core early in Mercury's history (Solomon, 1976), even small quantities of light alloying elements, such as sulfur or oxygen, could have prevented the core from freezing (Stevenson *et al.*, 1983). An active hydrodynamic (Stevenson, 1983) or thermoelectric dynamo (Stevenson, 1987; Giampieri and Balogh, 2002) operating at Mercury is, therefore, a strong possibility.

Thermoremanent magnetization of the crust may have been induced either by a large external (i.e., solar or nebular) magnetic field or by an internal dynamo that existed earlier in the planet's history. The former possibility is implausible because any early solar or nebular field would presumably have decayed much faster than the timescale for thickening of Mercury's lithosphere (Stevenson, 1987). The latter hypothesis of an early dynamo as the source for thermoremanent magnetization at Mercury faces additional requirements set forth by the magnetostatic theorem of Runcorn (1975a,b). Runcorn showed that the symmetry of the magnetic field due to thermoremanent magnetization of a uniform, thin shell by a formerly active internal dynamo at the planet's center does not produce a magnetic field external to the planet. However, Runcorn's theorem is valid only under several ideal conditions, including (1) the permeability of the magnetizedq shell was uniform (Stephenson, 1976), (2) the cooling of the planetary interior occurred from the outermost layer progressively inward (Srnka,

1976), and (3) the thermal structure of the lithosphere exhibited no asymmetries during the cooling process (Aharonson *et al.*, 2004). Breaking any of the above stringent conditions could result in a net planetary magnetic moment. Hence, crustal magnetization cannot be excluded as a source for some or all of Mercury's planetary magnetic field.

## 4.2 HOW WILL MESSENGER MEASUREMENTS BE USED TO DETERMINE THE ORIGIN OF MERCURY'S INTRINSIC MAGNETIC FIELD?

Determining the origin of Mercury's magnetic field is one of MESSENGER's prime objectives. The approach to addressing this objective will be to produce an accurate representation, or "map", of Mercury's intrinsic magnetic field and use it to distinguish among the several hypotheses for the origin of Mercury's magnetic field. This process, combined with the MESSENGER gravity and altimetry investigations, should ultimately yield considerable insight into the interior structure and evolution of this small planet. Clues to the origin of the planetary magnetic field are expected to be found in the multipole decomposition of the planetary field, which will be retrieved from an inversion of the magnetic field measurements.

The principal external current systems are the magnetopause current that confines much of the magnetic flux originating in the planet to the magnetospheric cavity and the cross-tail current layer that separates the two lobes of the tail. A "ring current" due to the drift motion trapped of energetic ions and electrons, observed at Earth during geomagnetic "storms", is not expected because of the absence of closed drift paths in Mercury's magnetosphere. Slavin *et al.* (1997), however, did report evidence for the existence of high-latitude field-aligned currents at Mercury, but owing to the absence of a conducting ionosphere, their structure may differ greatly from those at Earth. Two methods of accounting for the external field contribution in the inversion are typically used. In the first, a spherical harmonic expansion series is used in which the external field is treated by adding a scalar potential function. Whether a scalar representation best captures the external contribution is not clear. The second approach applies our present understanding of magnetospheric current systems to model the individual magnetospheric current systems and subtract their contribution prior to evaluating the structure of the intrinsic field. Several works have established geometric descriptions of the magnetic fields due to magnetopause currents and tail currents in the Earth's magnetosphere, which have been successfully adapted to Mercury's magnetosphere (Whang, 1977; Korth *et al.*, 2004). Our ability to characterize reliably the structure of Mercury's intrinsic magnetic field is, therefore, determined by the extent to which the external field can be understood and accurately modeled.

The extended spatial coverage of the MESSENGER observations yields a number of important benefits. First, the residuals remaining after fitting for different external field conditions will vary more distinctively, thus allowing better determination of the quality of the inversion solutions. Second, cross-correlation among the

spherical harmonic coefficients will be significantly reduced; allowing for the derivation of improved quasi-linearly independent higher-order moments of the field representation. Simulations of the magnetic field environment at Mercury have shown that the dipole moment should be recoverable to within 10% without applying any corrections for the external field (Giampieri and Balogh, 2001; Korth *et al.*, 2004). Further, the magnetic field data will provide significant clues about the occurrence of dynamic magnetospheric processes, so it will be possible to pre-select the data to be included in the inversion and reduce dynamic effects to a minimum. It is expected that the most reliable solutions will be afforded by the most carefully chosen "northward IMF - non-substorm" observations when the external conditions are weakest. We expect that the ultimate accuracy will be determined by a trade-off between statistical uncertainty, which grows as the number of observations is reduced, and systematic error, which decreases as the data are more carefully selected. In any case, the ultimately achievable accuracy for the dipole term will be fairly high, on the order of a few percent, and many higher-order terms should also be reliably recovered.

Additional analyses will relate to the fine structure of Mercury's crustal magnetic field. The altitudes of the MESSENGER orbit in the northern hemisphere are sufficiently low (200-km minimum altitude) that field structures due to crustal anomalies, if present, can be directly mapped if present. Large crustal remanent fields were found at Mars (Acuna *et al.*, 1998; 1999) and may also be present at Mercury, although the carriers of the remanence and the internal field history are probably different for the two bodies. If only those magnetic features having a lateral extent larger than the spacecraft altitude can be resolved, then the effective longitudinal and latitudinal resolution is determined by the spacecraft orbit. Accordingly, we expect to be able to resolve magnetic features with horizontal dimensions of 5° (about 200 km) near the periaspsis latitude.

### 4.3 HOW, WHEN, AND WHERE DOES THE SOLAR WIND IMPACT THE PLANET?

The manner, flux, energy spectrum, and location of solar wind and solar energetic particle (SEP) impact upon the surface is important because of the role that these processes play in sputtering neutrals out of the regolith into the exosphere and their contribution to changing the appearance and physical properties of the surface (Killen *et al.*, 1999; 2001; Lammer et al., 2003; Sasaki and Kurahashi, 2004). Solar wind and SEP charged particles may intercept the surface by two mechanisms. First, finite gyroradius effects can result in ions being lost to collisions with regolith material wherever the strength of the magnetospheric magnetic field and the height of the magnetopause is such that their centers of gyration are within one Larmor radius of the surface (Siscoe and Christopher, 1975; Slavin and Holzer, 1979a). Second, "open" magnetospheric flux tubes with one end rooted in the planet and the other connected to the upstream interplanetary magnetic field will act as a "channel" that guides charged particles down to the surface, except for those that "mirror" prior to impact with the regolith (Sarantos, 2000; Massetti et al., 2003).

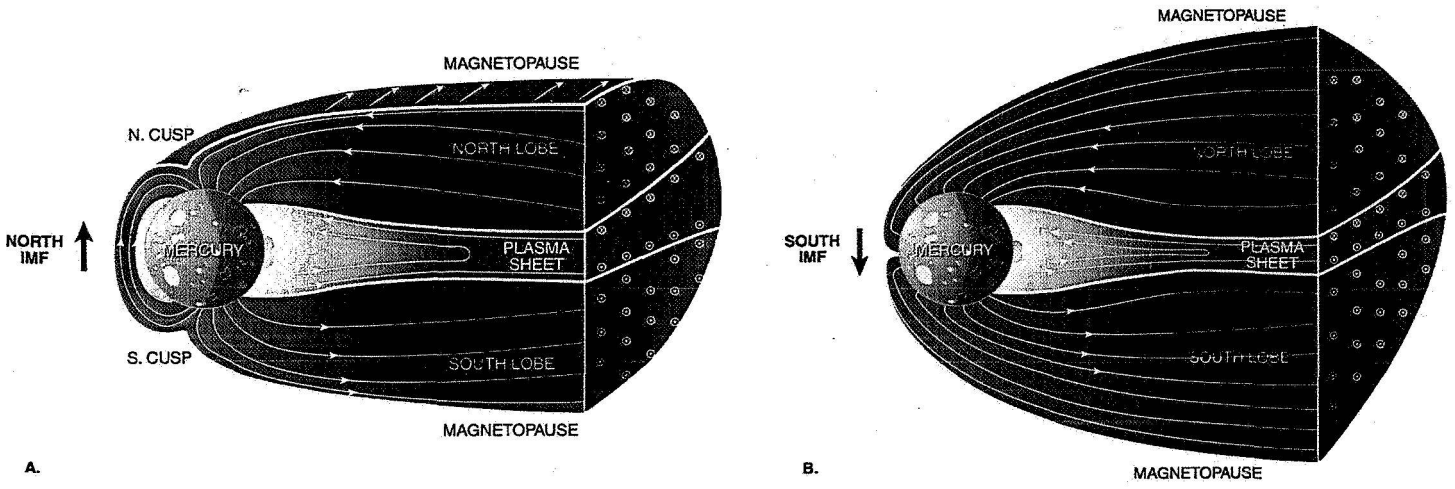


Figure 5. Schematic view of the magnetosphere of Mercury. Regions with low plasma temperature (solar wind and tail lobes) are colored blue while the hotter regions (inner magnetosphere and plasma sheet) are shown in redder hues. The two images illustrate the extreme cases of minimal (A) and maximal (B) tail flux expected for northward and southward interplanetary magnetic field, respectively.

An idealized view of Mercury's magnetosphere under a northward interplanetary magnetic field (IMF), based on the Mariner 10 measurements, is presented in Figure 5a. It has been drawn using an image of the Earth's magnetosphere and increasing the size of the planet by a factor of ~ 7 - 8 to compensate for the relative weakness of the dipole field and the high solar wind pressure at Mercury (Ogilvie *et al*; 1977). The mean ~1.5 $R_M$ distance from the center of Mercury to the nose of the magnetosphere inferred from the Mariner 10 measurements (Siscoe and Christopher, 1975; Ness *et al.*, 1976; Russell, 1977; Slavin and Holzer, 1979a) corresponds to 10 - 11 $R_E$ where $R_E$ is the Earth's radius and 1 $R_E$ = 6378 km.

Whether or not the solar wind is ever able to compress the dayside magnetosphere to the point where solar wind ions directly impact the surface at low latitudes remains a topic of considerable interest and controversy. Siscoe and Christopher (1975) were the first to take a long time series of solar wind ram pressure data taken at 1 AU, scale it by $1/r^2$ inward to Mercury's perihelion, and then compute the solar wind stand-off distance using a range of assumed planetary dipole magnetic moments. They found that only for a few percent of the time would the magnetopause will be expected to fall below an altitude of ~ 0.2 $R_M$, the point where solar wind protons begin to strike the surface due to finite gyro-radius effects.

Rapid large-amplitude changes in solar wind ram pressure associated with high-speed streams and interplanetary shocks might be expected easily to depress the magnetopause close to the surface of planet. However, it is expected that induction currents will be generated in the planetary interior (Hood and Schubert, 1979; Suess and Goldstein, 1979; Goldstein *et al.*, 1981; Glassmeier, 2000; Grosser *et al.*, 2004) and that these currents will act to resist rapid magnetospheric compressions. Model predictions suggest that the ram pressure increase required to push the magnetopause to within 0.1 $R_M$ of the surface may be an order of magnitude more

than what would be required in the absence of induction effects. Mercury's interaction with the solar wind may, therefore, provide a unique opportunity to study this planet's large electrically conductive core via its inductive reactance to externally imposed solar wind pressure variations.

The "erosion," or transfer, of magnetic flux into the tail is well studied at Earth, where the distance to the subsolar magnetopause is reduced by ~ 10 – 20% during a typical interval of southward IMF (Sibeck *et al.*, 1991). Analysis of the Mariner 10 magnetopause and bow shock crossings, after scaling for upstream ram pressure effects, by Slavin and Holzer (1979a) indicated that the subsolar distances extrapolated from the individual boundary encounters varied from 1.3 to 2.1$R_M$, with the larger values corresponding to IMF $B_z > 0$ and the smaller to $B_z < 0$. Similar variations in dayside magnetopause height have been found in MHD simulations of Mercury's magnetosphere under southward IMF conditions by Kabin *et al.* (2000) and Ip and Kopp (2002). Further evidence that reconnection operates at Mercury's magnetopause comes in the form of the "flux transfer events" identified in the Mariner 10 data by Russell and Walker (1985). These flux rope-like structures have been studied extensively at the terrestrial magnetosphere where they play a major role in the transfer of magnetic flux from the dayside to the nightside magnetosphere.

In the limit that all of the magnetic flux in the dayside magnetosphere of Mercury were to reconnect quickly, then the north and south cusps are expected to move equatorward and merge to form a single cusp as displayed in Figure 5b. All of the flux north (south) of this single cusp will map back into the northern (southern) lobe of the tail. Direct solar wind impact on the surface will take place in the vicinity of the merged subsolar cusp. However, such extreme events are not necessary. As shown by Kabin *et al.* (2000) and Sarantos *et al.* (2001), the strong radial IMF near Mercury's orbit should always be conducive to solar wind and SEP particles being channeled to the surface along reconnected flux tubes that connect to the upstream solar wind. For the completely eroded dayside magnetosphere shown in Figure 5b, the solar wind and SEP charged particles would impact a large fraction of the northern (southern) hemisphere of Mercury for IMF $B_x > 0$ ($B_x < 0$). Whether or not the fully reconnected dayside magnetosphere shown in Figure 5b is ever realized will be determined by the rate of reconnection at the magnetopause and how long it takes for Mercury's magnetosphere to respond by reconnecting magnetic flux tubes in the tail and convecting magnetic flux back to the dayside. Slavin and Holzer (1979a) have argued that the high Alfven speeds in the solar wind at 0.3 to 0.5 AU may produce very high magnetopause reconnection rates and lead to strong erosion of the dayside magnetosphere even if the timescales for the magnetospheric convection cycle is only ~ 1 – 2 min.

## 4.4 HOW WILL MESSENGER DETERMINE THE EXTENT OF SOLAR WIND IMPACT?

The two critical factors controlling the impact of the solar wind and SEP particles to the surface are the height of the magnetopause, and the distribution of "open" magnetic flux tubes that are topologically connected

to the upstream region. MESSENGER will encounter and map the principal magnetospheric boundaries and current sheets, i.e., the bow shock, magnetopause, magnetic cusps, field-aligned currents, and the cross-tail current layer, throughout the mission. Typically, these surfaces are modeled by identifying "boundary crossings" and then employing curve fitting techniques to produce 2- or 3-dimensional surfaces. If such encounters can be collected for a variety of solar wind and magnetospheric conditions, then parameterized models may be produced. The essential requirement for this technique to be successful is the availability of crossings over a wide range of local times and latitudes along trajectories that provide good spatial coverage above and below the mean altitude of the surfaces (e.g., see Slavin and Holzer, 1981). Inspection of the first Mercury-year of MESSENGER orbits, displayed in Figures 3a and b, indicates that the modeling of bow shock, magnetosphere, and cross-tail current layer using boundary crossings should work very well sunward of X ~ -3.5 $R_M$. The lack of coverage of the northern halves of the bow shock and magnetopause surfaces should not be a significant problem because of the expected symmetry between the two hemispheres. The models of the magnetopause and magnetic cusps will be used to infer the extent and frequency with which the magnetopause altitude becomes so low that a given population of interplanetary charged particles may find itself within one Larmor radius of the surface.

However, the measurements of the charged particle distribution functions and pitch angle distributions by the FIPS and EPS sensors when MESSENGER is within the magnetosphere will provide the most direct information regarding the ion and electron fluxes reaching the surface of the planet. Charged particles on magnetic flux tubes that connect to the planet will be lost if their magnetic mirror points are below the surface of the planet. This effect produces a "loss cone" signature in the particle pitch angle distributions, which is a definitive indication of particles impacting the surface. The EPPS instrument will return charged particle distribution functions according to particle composition, charge state, and energy that will be inverted to infer the flux of particles impacting the surface of Mercury. The results are expected to vary greatly depending upon where the spacecraft is located, the topology of the local magnetic field, and the state of the magnetosphere (i.e., IMF direction and substorm vs. non-substorm conditions).

## 5. Magnetospheric Dynamics

### 5.1 WHAT ARE THE PRINCIPAL MECHANISMS FOR CHARGED PARTICLE ACCELERATION AT MERCURY?

Charged particle acceleration is one of the most fundamental processes occurring in space plasmas. Planetary magnetospheres are known to accelerate particles from thermal to high energies very rapidly via a range of processes. The plasma in Mercury's magnetosphere is expected to come from two sources, the solar wind and the ionization of the neutral exosphere. Solar wind plasma enters the magnetosphere by flowing along

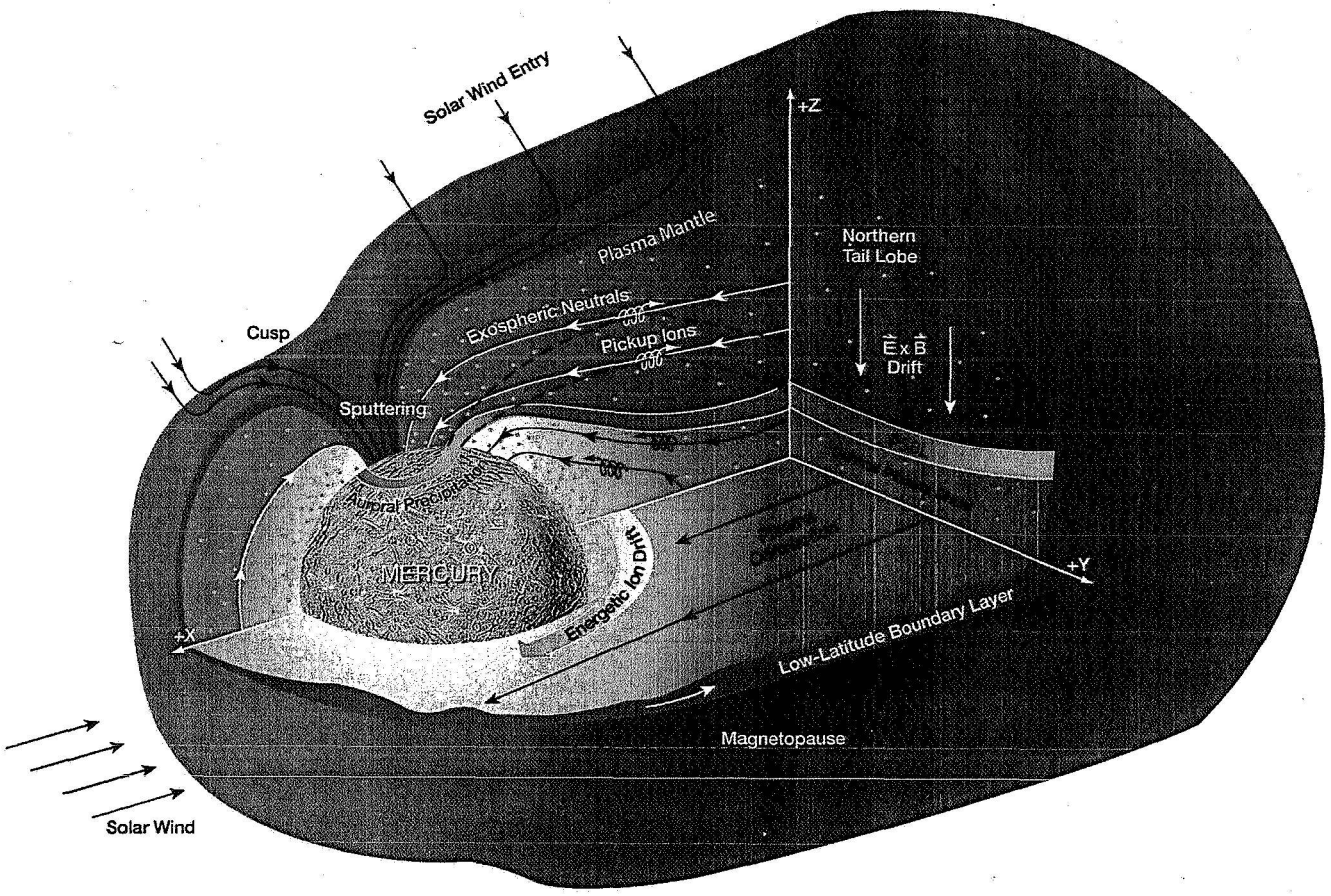


Figure 6. Magnetospheric convection and the pick-up of newly ionized exospheric particles. Note the relatively straight equatorial convection paths expected at Mercury due to the planet's extremely slow rotation rate.

"open" flux tubes that connect to the interplanetary medium as shown in Figure 6. After reconnection splices together an interplanetary and a planetary flux tube, the solar wind particles are channeled down into the cusp region where either they either mirror and reverse their direction of motion or they impact the regolith and are absorbed. The solar wind particles that mirror and then flow tailward now find themselves in the "plasma mantle" region of the tail. Due to the dawn-to-dusk electric field that the solar wind interaction impresses across the magnetosphere, the plasma in the mantle will "E x B" drift toward the equatorial regions of the tail where it will be assimilated into the plasma sheet. Delcourt *et al.* (2003) showed that the large Larmor radii of the newly created sodium ions will result in significant "centrifugal" acceleration as the ions E x B drift at lower altitudes over the polar regions of Mercury. Similarly, at higher altitudes Delcourt *et al.* found that these large Larmor radii will result in ion motion that is generally non-adiabatic and "Speiser-type" trajectories near the cross-tail current layer with the ions rapidly attaining energies of several keV. The neutral species in the exosphere travel on ballistic trajectories determined only by gravity and light pressure until the point where they become ionized

by solar ultraviolet (UV) radiation, charge exchange with a magnetospheric ion, or electron impact ionization. At that point the new ion will begin to execute single particle motion according to its velocity vector at the time of creation and the ambient electric and magnetic fields within the magnetosphere (Cheng et al., 1987; Ip, 1987; Delcourt *et al.*, 2002; 2003). Alternatively, some of the ions may possess sufficiently large Larmor radii to intersect quickly the magnetopause and be lost. For those pickup ions remaining in the magnetosphere, plasma waves will be excited and grow at the expense of their kinetic energy until the ions become "thermalized," are lost to impact on the planet, or drift to the magnetopause. Since Mercury takes 59 days to spin once about its axis, planetary rotation is not expected to play any role in particle acceleration or transport. Hence, the E x B drift or "convection" path for magnetospheric plasma is expected to follow relatively straight lines from the plasma sheet sunward toward the nightside of the planet or the forward magnetopause, as shown in Figure 6.

Some of the most energetic charged particles in the tail are thought to be accelerated by the intense electric fields driven by the reconnection of magnetic flux tubes from the lobes of the tail (Hill, 1975). At Earth, recently reconnected flux tubes are observed to be bounded by "magnetic separatrices" (Cowley, 1980; Scholer *et al.*, 1984) populated with newly accelerated ions and electrons. The particles possessing the highest $V_{parallel}$ are found farthest from the current sheet and closest to the separatrix boundary. These regions of sunward and tailward streaming energetic charged particles are colored red in Figure 7. Indeed, short lived, "spikes" in energetic ions and electron flux extending up to at least several MeV have been seen in Earth's distant magnetotail (Krimigis and Sarris, 1979) and have been associated with episodes of X-line formation and reconnection (Sarris and Axford, 1979; Richardson *et al.*, 1996). Non-adiabatic processes are necessary to explain these acceleration events, usually attributed to the effect of extreme thinning of the cross-tail current sheet relative to the Larmor radii of the ions and electrons (Buchner and Zelenyi, 1989; Delcourt *et al.*, 2003; Hoshino, 2005).

Many of these accelerated charged particles are immediately lost as they flow down the tail to the interplanetary medium. Others, however, are carried sunward and undergo further acceleration due to first invariant conservation. At Earth, ions convected from the inner edge of the tail may have their energy increased by a factor of 100 by the time they reach the "ring current" region at a radial distance of ~ 3 $R_E$ from the center of the planet. By contrast, the weak planetary magnetic field at Mercury greatly limits this type of convection-driven acceleration. Indeed, Mercury may be ideal for the direct observation of acceleration associated with X-line formation. As these charged particles approach Mercury and experience stronger magnetic fields, the ions and electrons will begin to experience gradient and curvature drift that cause the ions to drift about the planet toward dusk while electrons are diverted toward dawn, as indicated in Figure 6. The loss of these energetic particles via intersection with the surface of Mercury or the magnetopause is expected to severely limit the flux

of quasi-trapped particles that complete a circuit about the planet (Lukyanov *et al.*, 2001; Delcourt *et al.*, 2003), but their loss constitutes an additional source of surface sputtering.

Charged particles also experience acceleration during interactions with ULF waves (e.g., Blomberg, 1997). Ion pickup due to photo-ionization of neutrals sputtered from the surface is expected to be a persistent feature of Mercury's magnetosphere (Ip, 1987). These newly created ions will then experience the convection electric field and be picked up in the plasma flow much as newly ionized atoms are swept up in the solar wind flow near comets (e.g., Coates *et al.*, 1996). The resulting pickup ion distributions contain significant free energy and can be unstable to various cyclotron wave modes, many of which have magnetic signatures in the vicinity of the ion gyro-frequencies (Gomberoff and Astudillo, 1998). Cyclotron waves may also be generated by ions accelerated in the magnetotail as they convect sunward and are commonplace at Earth (Anderson *et al.*, 1992). At Earth ion populations can also drive long-wavelength, low-frequency waves which, in turn, couple to field-line resonances (e.g., Southwood and Kivelson, 1981). While the ion gyro-frequencies and field-line resonance frequencies at Earth are separated by a factor of 10 to 100, at Mercury the gyro-frequencies are fairly low because of the low magnetic field strength at Mercury, while the field line resonance periods should be relatively high owing to the small size of the magnetosphere (Russell, 1989). The wave-particle physics at Mercury may, therefore, be particularly interesting, because the kinetic and longer wavelength waves should be coupled (Glassmeier *et al.*, 2003).

## 5.2 HOW WILL ENERGTIC PARTICLE ACCELERATION PROCESSES BE MEASURED AT MERCURY?

The EPPS and MAG instruments will be used in concert to explore Mercury's magnetosphere, map out its different regions, and determine the spatial and temporal variations in the charged particle populations peculiar to the different parts of the magnetosphere (see Mukai *et al.*, 2004). For example, the magnetic field and plasma measurements will be used to calculate the ratio of thermal particle pressure to magnetic pressure, termed the "beta" value of the plasma. The inner regions close to the planet and the lobes of tail are typically dominated by the magnetic field pressure and have very low beta values, i.e., $< 0.1$. The plasma sheet region (see Figure 6), in contrast, is dominated by thermal pressure. At Earth the plasma sheet has beta values that vary from a few times 0.1 in the outer layers to $>> 10$ in the central portion where the cross-tail electric current density peaks. The most dynamic events observed in the Earth's magnetosphere, such as "bursty bulk flows" and "dipolarizations," are generally found in the plasma sheet region. Streaming energetic particles accelerated in the separatrices X-lines are most frequently observed in the outer layers of the plasma sheet where beta ~ 0.1.

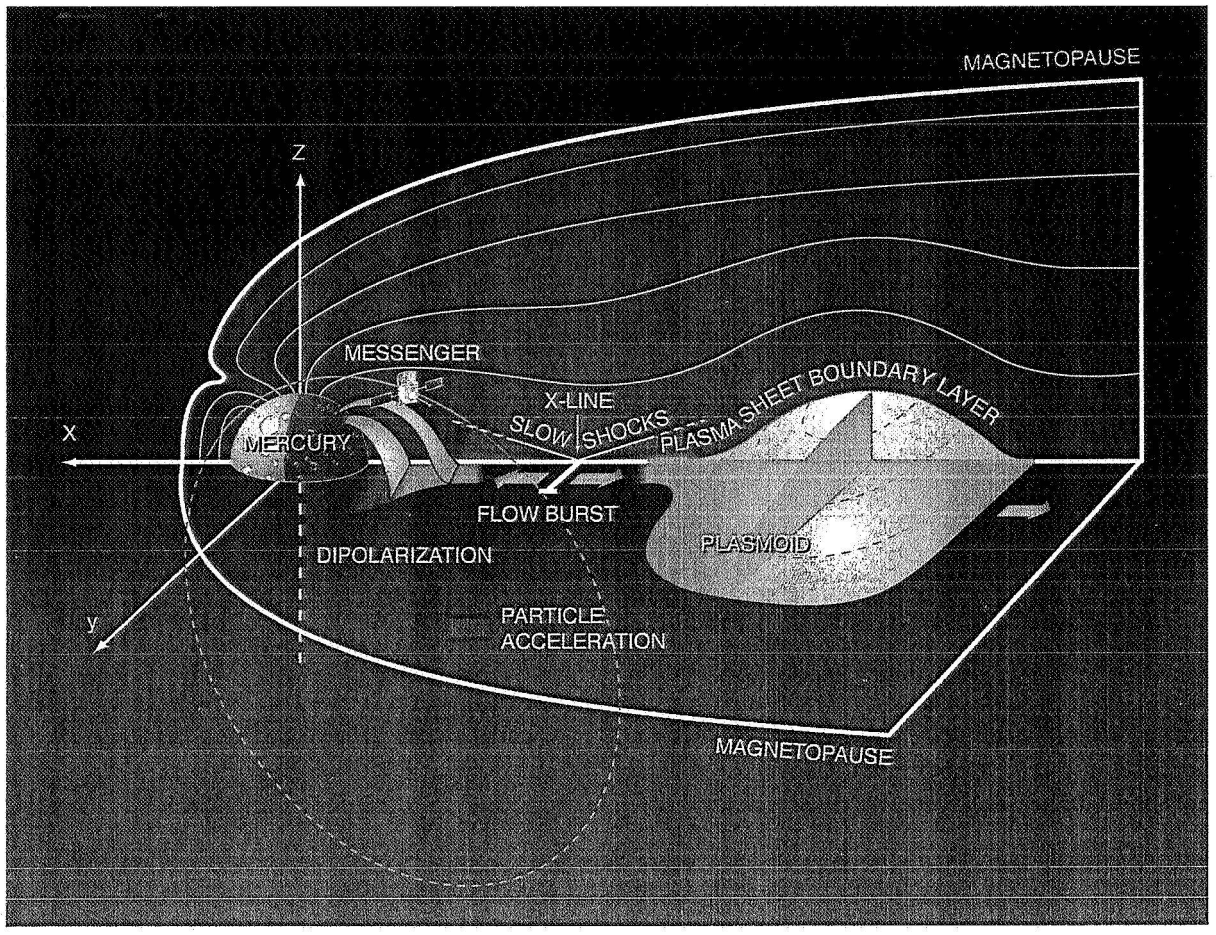


**Figure 7**. Schematic depiction of a reconnection-driven substorm within Mercury's magnetosphere

The MESSENGER EPPS instrument will provide comprehensive observations of ions and electrons from low altitudes over the north polar regions (see Figure 3b) out through the lobes and into the cross-tail current layer. The exchange of mass between the surface of the planet and the magnetosphere will be directly measured and the attendant acceleration of the charged particles will be observed. The natural tendency of energetic particles to disperse, with faster particles reaching an observer before the slower particles, is a strong modeling constraint for determining the source populations, drift paths and magnetic conjugacies. Modeling and analysis of dispersed ion-injection events at various distances down the tail at the Earth have shown that it is often possible to specify the time and location where the initial acceleration event took place (Mauk, 1986; Sauvaud *et al.*, 1999; Kazama and Mukai, 2005).

The MESSENGER magnetometer is also designed to characterize waves and wave-particle interactions at Mercury. The MAG instrument provides coverage up to 10 Hz a band that spans all of the relevant ion gyro-frequencies including protons throughout the planetary magnetosphere. Even during periods of low telemetry allocations the magnetospheric sampling will be no coarser than 2 vectors $s^{-1}$ providing coverage over all ulta-low frequency (ULF) and heavy-ion gyro-frequencies. Moreover, the MAG provides a burst detection capability

that will allow capture of large-amplitude wave events. In concert with FIPS and EPS observations of ion distributions and composition such measurements will provide a comprehensive survey of wave activty and determine their correspondence with the local ion populations.

## 5.3 DO TERRESTRIAL-STYLE SUBSTORMS OCCUR AT MERCURY?

Mercury is expected to be one of the best places to test and extend our understanding of magnetospheric substorms. Because of its closeness to the Sun, this magnetosphere is subject to the most intense solar wind pressure and IMF intensity in the solar system (Burlaga, 2001). The MESSENGER measurements will give detailed observations of substorms in a magnetosphere where planetary rotation is negligible and no ionosphere is present. The slow rotation of Mercury will result in sunward convection being dominant throughout the near-planet magnetosphere. This is in stark contrast with Saturn, the other planet where terrestrial-type substorms are thought to occur. Saturn has a rapid rotation that dominates convection in the forward magnetosphere that may even twist the tail magnetic field into a helical configuration (Mitchell *et al.*, 2005; Cowley *et al.*, 2005).

The absence of a collisional ionosphere at Mercury also has important consequences for global electric currents and plasma convection within this small magnetosphere. At Earth and Saturn it is believed that the timescale for the substorm growth phase is determined by ionospheric line-tying that in turn limits the rate of magnetic flux circulation from the dayside magnetosphere to the nightside and back again (Coroniti and Kennel, 1973). Furthermore, some theories of the substorm expansion phase at Earth require active feedback between the magnetosphere and an ionosphere whose conductivity varies at least somewhat with the rate of charged particle precipitation (Baker *et al.*, 1996). Such feedback is presumably absent at Mercury, although we shall evaluate the situation using the MESSENGER observations. In this manner, it will be determined whether or not active feedback between an ionosphere and the equatorial magnetosphere is a necessary condition for magnetospheric substorms. Finally, the flow of field-aligned currents to low altitudes produces auroras in the Earth's upper atmosphere when the charge carriers impact neutral atoms and produce visible and UV emissions. It is unlikely that classical auroras would occur at Mercury. Nonetheless, the closure of magnetospheric currents through the near-surface of Mercury may create a "warm" (i.e., "less cold") "auroral" band at the surface due to Joule dissipation (Baker *et al.*, 1987), as shown in Figure 6.

Siscoe *et al.* (1975) and Ogilvie *et al.* (1977) showed that the energetic particle bursts detected by Mariner 10 tended to occur at times when the magnetic field exhibited the disturbed behavior characteristic of substorms at Earth. Mariner 10 entered the near-tail plasma sheet on the dusk side of the tail during its first Mercury encounter. The magnetic field observed inside the magnetopause was very tail-like and relatively quiet during the inbound half of the encounter. Shortly after closest approach, $|\mathbf{B}|$ decreased rapidly, and the field inclination increased markedly, becoming less tail-like and more dipole-like. Such magnetic field variations are

a classic signature of substorm expansive phase onset at the Earth (Baker *et al.*, 1996) where they are termed "dipolarization events." Christon *et al.* (1987) conducted comparative studies of the magnetic field changes observed in association with the Mercury and Earth magnetosphere energetic particle events in the near-tail and found them to be extremely similar.

Siscoe *et al.* (1975) also called attention to the fact that the IMF switched from northward to southward while Mariner 10 was in the magnetosphere. These authors suggested, by analogy to Earth, that this change in IMF direction initiated reconnection at the dayside magnetopause, magnetic flux transfer to the tail, and, finally, tail reconnection. As shown schematically in Figure 7, tail reconnection is believed to drive fast plasma flows and energetic particle acceleration. Indeed, Slavin and Holzer (1979a) found that the altitude of the dayside magnetopause for both M10 encounters was reduced whenever the IMF $B_z$ component was southward, consistent with the reconnection model. Siscoe *et al.* further used scaling arguments to suggest that if substorms occurred at Mercury, then the timescales should be of order 1-2 min, similar to the M10 energetic particle events, as compared with the ~ 1 hr typical of the Earth's magnetosphere.

Eraker and Simpson (1986) and Baker *et al.* (1986) developed this scenario further and suggested that the substorms in Mercury's magnetotail resulted from magnetic reconnection in the range of 3-6 $R_M$ on the nightside, as shown in Figure 7. During substorms in Earth's magnetosphere, the plasma sheet has been observed to be severed by magnetic reconnection quite close to Earth, i.e., ~ 20 – 30 $R_E$ or ~ 2 – 3 times the solar wind stand-off distance. The reconnection process produces a magnetically confined structure (i.e., loop-like or helical magnetic topology) termed a "plasmoid" (Hones *et al.*, 1984) that is ejected down the tail at high speed, as schematically depicted in Figure 7. As at the Earth, the observation of plasmoids in Mercury's magnetotail would provide direct information regarding the time of onset and intensity of magnetic reconnection (e.g., Baker *et al.*, 1987; Slavin *et al.*, 2002).

## 5.4 HOW WILL SUBSTORM ACTIVITY BE IDENTIFIED IN THE MESSENGER MEASUREMENTS?

Given our present understanding of the Mariner 10 observations, we expect that substorms in the MESSENGER data will appear whenever the IMF upstream of Mercury becomes persistently southward. When the spacecraft is located in the tail lobes on the night side of Mercury, MAG should measure increases in the magnetic field strength and a "tail-like" stretching of the field lasting for some tens of seconds. We expect these energy storage or "growth" phases (McPherron *et al.*, 1973) would be soon followed by one or more rapid dipolarizations of the magnetic field. If MESSENGER finds itself on the sunward side of the site for magnetic reconnection in Mercury's magnetotail, there should be strong sunward plasma flow and intense energetic particle bursts. On the other hand, if MESSENGER were located tailward of the magnetic reconnection site, then strong anti-sunward plasma flow and magnetic signatures of plasmoids, or flux ropes are anticipated

(Figure 7). However, it would not be surprising if the small dimensions of this magnetosphere produce some unique and unexpected substorm features.

Beyond these basic expectations, there are many important "system response" characteristics that will be determined. For example, substorms at Earth are known to exhibit both "driven" responses that can be predicted using linear "filters" and knowledge of the upstream solar wind and IMF (Bargatze *et al.*, 1985) and an unpredictable, "spontaneous" component related to the magnetic energy stored in the lobes. Lacking a conductive ionosphere, it may be that Mercury's magnetosphere cannot store significant amounts of energy and the spontaneous component of substorm energy dissipation will be small or absent (Luhmann *et al.*, 1998). In this case MESSENGER's magnetic field and charged particle instruments may frequently observe "continuous dissipation events" in the tail that are directly driven by the solar wind. At Earth, in contrast, this type of intense, relatively featureless magnetospheric convection is seen only in response to many hour long intervals of intense, strongly southward IMF (Tanskanen *et al.*, 2005).

We also expect to use the Mercury Atmospheric and Surface Composition Spectrometer (MASCS) instrument to study key aspects of the solar wind-magnetosphere-exosphere interaction. This spectrometer is described in a companion article (McClintock *et al.*, 2005). As portrayed in Figure 6, the strong dissipation of energy in substorm-like events at Mercury is expected to produce powerful bursts of plasma and energetic particles directed along magnetic field lines down onto the cold nightside surface of Mercury (Baker *et al.*, 1987). It is part of our observation strategy with MESSENGER to use the infrared detection capabilities of MASCS to look for evidence of heating of the nightside regolith of Mercury due to substorm energy precipitation.

## 6. Magnetosphere – Planetary Coupling

### 6.1 HOW MUCH MASS IS "RECYCLED" BETWEEN THE REGOLITH, EXOSPHERE AND MAGNETOSPHERE?

Extensive analysis and modeling have been devoted to the investigation of how ion impact sputtering, aided by solar radiation, may result in the injection and acceleration of newly created ions followed by further re-circulation, as diagrammed in Figure 8 (Ip, 1987; Killen *et al.*, 2001; Delcourt *et al.*, 2003). Trajectory analyses conducted by Killen *et al.* (2002) indicate that perhaps 60% of these photo-ions may subsequently impact the surface, where they are adsorbed and become available for release via sputtering and impact vaporization. Furthermore, if reconnection at the dayside magnetopause frequently exposes significant fractions of the surface directly to impact by charged particles from the interplanetary medium, then the contribution of neutrals sputtered by solar wind ions (Sarantos *et al.*, 2001) and solar energetic particles (Leblanc *et al.*, 2003) to the exosphere may be a major driver for this system. The relatively short times required

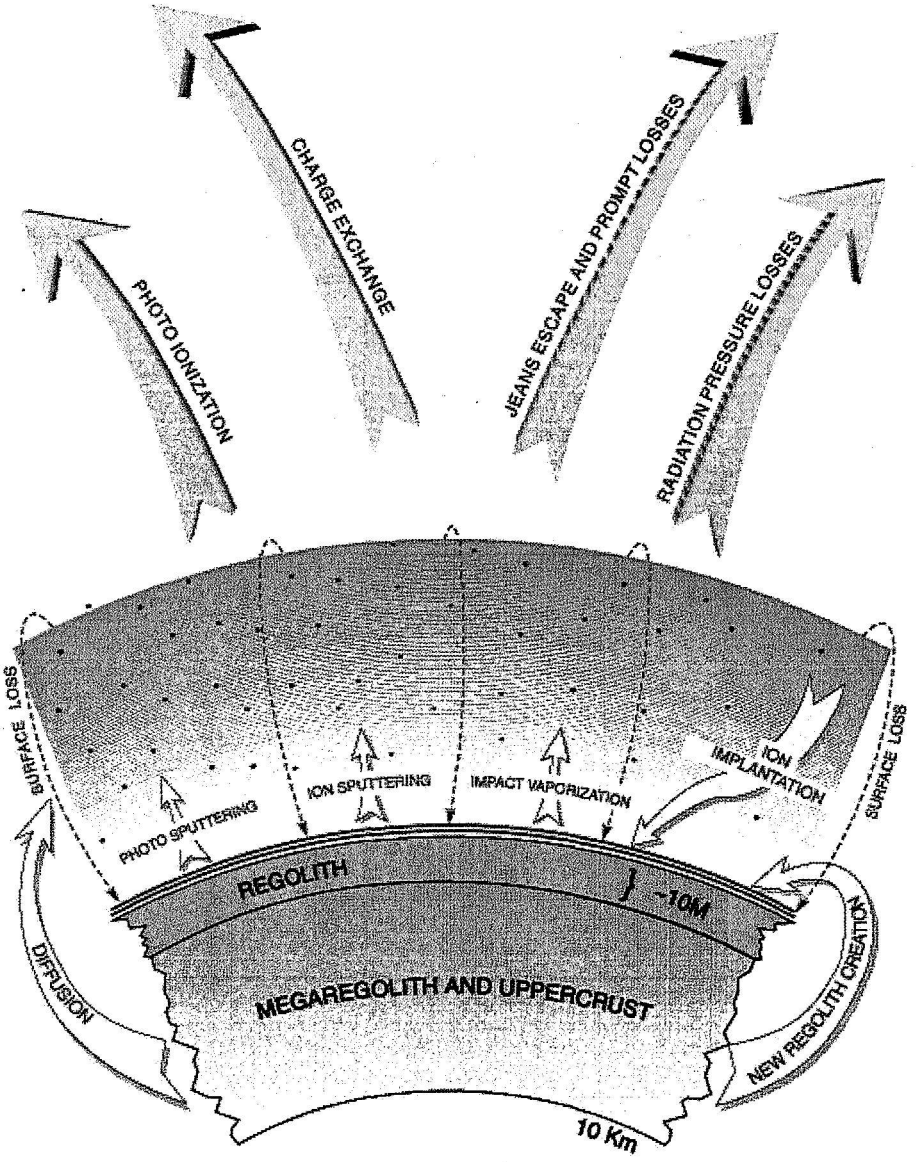


Figure 8. Mass exchange between the solar wind, magnetosphere, exosphere, and regolith at Mercury (Killen, 2001).

for photo-ionization and charge exchange will lead to sputtered neutrals being quickly ionized and picked-up by the convective flow within the magnetosphere to produce a closely coupled system (see also Figure 6).

The nature of this complex chain of coupled processes that link the planet to the atmosphere and the magnetosphere has become a major focus for the Mercury research community. Killen *et al.* (2001) found that Mercury's atmosphere is sufficiently tenuous that it would soon be depleted by losses associated with photo-ionization and charge exchange, if it were not being continuously replenished from above and below as depicted in Figure 8. The creation of exospheric neutrals involves four competing processes: photo-sputtering, thermal

desorption, particle sputtering and meteoric impact (e.g., Killen and Ip, 1999; Milillo *et al.*, 2005). All of these processes and how the MESSENGER measurements will contribute to our understanding of them are discussed in detail in a companion article by Domingue *et al.* (2005).

The dynamic nature of Mercury's magnetosphere is expected to complicate the measurement of the rate of recycling of magnetospheric ions and neutrals. The exospheric neutrals available for ionization depend heavily on the composition of the planetary surface. Charged particle and photon sputtering work on the first few monolayers of the surface grains, so pre-sputtered atoms must first make their way to the monolayers by diffusion. Gardening rates for the crust are much faster than the time required to deplete a grain of a given species, providing a constant supply of neutrals to the exosphere (Killen *et al.*, 2004). Based upon the Mariner 10 observations, the magnetospheric reconfiguration time is only a few minutes (Siscoe *et al.*, 1975; Slavin and Holzer, 1979a; Luhmann *et al.*, 1998). Hence, the trajectories of magnetospheric ions through the magnetosphere may be quite complex (Delcourt *et al.*, 2002). After a newly liberated neutral leaves the surface, it follows a ballistic trajectory until one of several events happen (see review by Hunten *et al.*, 1988). The neutral can become ionized, in which case it is accelerated by the magnetospheric electric fields until it either collides with the planetary surface or is thermalized and swept sunward or tailward by the convective flow in the equatorial magnetosphere.

Several studies have been performed that examine the importance of ion recycling in Mercury's exosphere and magnetosphere (e.g., Zurbuchen *et al.*, 2004). Koehn (2002) used the MHD model of Kabin *et al.* (2000) to study the surface-to-surface transport of $OH^+$ and $S^+$ ions. For normal solar wind conditions, he found that ions created at mid-latitudes tended to return to equatorial dusk regions, while ions formed elsewhere were lost to the magnetosphere and solar wind. For very strong solar wind conditions, returning ions tended to move poleward and duskward, enhancing mid-latitude regions. Recycling rates for this study were less than 10%.

Delcourt *et al.* (2003) and Leblanc *et al.* (2003) followed the trajectories of $Na^+$ ions with an initial energy of 1 eV using a realistic magnetospheric magnetic field model. Their results show $Na^+$ returning to the surface primarily along two mid-latitude regions centered on $\pm 30^\circ$, with some returning to duskside latitudes of less than $20^\circ$. Recycling rates for these studies were 10-15%. Killen *et al.* (2004) utilized a new model (see Sarantos 2000) that, unlike Delcourt *et al.* (2003), takes into account radial magnetic field orientation. Their ion initial energies were also ~1 eV. The measured recycling rates are significantly higher (60%), and they find that dawnside-generated ions tend to return to the surface, while duskside born ions are swept away by the solar wind.

## 6.2 HOW WILL THE MESSNENGER OBSERVATIONS BE USED TO DISCOVER THE EXTENT OF THE MASS EXCHANGE BETWEEN MERCURY'S REGOLITH, EXOSPHERE AND MAGNEOTSPHERE?

Perhaps no science objective will so fully utilize the MESSENGER instruments as the study of the mass exchange between the planetary surface, exosphere, and magnetosphere. The MAG instrument will map the magnetic field, providing insight into magnetospheric dynamics and supporting improved field models. The Gamma-Ray and Neutron Spectrometer (GRNS) and X-Ray Spectrometer (XRS) instruments (Goldstein *et al.*, 2005; Schlemm *et al.*, 2005) will provide elemental composition maps of the surface, from which exospheric neutrals arise, forming the seed population for magnetospheric ions. MASCS will measure the composition of the neutral atmosphere, recently liberated from the regolith. EPPS will detect pickup ions in the magnetosphere and then map detected ions back to surface regions from which they escaped. The Mercury Dual Imaging System (MDIS) instrument (Hawkins *et al.*, 2005) will then image the surface from which these neutrals and ions are sputtered, thereby tying atmospheric and magnetospheric measurements back to surface features.

In addition, EPPS and MAG will allow us to understand the complex interplay between magnetospheric plasmas and the magnetic field. In the event that the magnetopause is compressed sufficiently such that the solar wind can come into direct contact with much of the surface, EPPS will monitor the likely large increase in magnetospheric ions. This large flux of ionized particles will modify the magnetospheric configuration on a local scale, which MAG will also detect. In summary, most aspects of the recycling of magnetospheric ions between the exosphere and surface are still very much open issues. The MESSENGER instrument payload will make the critical measurements that will resolve the most important questions regarding the mass exchange within this closely coupled system.

## 6.3 DO FIELD-ALIGNED CURRENTS COUPLE MERCURY TO ITS MAGNETOSPHERE AND HOW DO THEY CLOSE?

Among the fundamental aspects of all planetary magnetospheres visited thus far are field-aligned electric currents (Kivelson, 2005). When magnetospheric magnetic fields reconnect with the IMF and are pulled back into the tail, sheets of field-aligned current, termed "Region 1" currents, flow down into the high-latitude ionosphere on the dawn side of the polar cap and outward on the dusk side. These Region 1 currents are also expected to present at Mercury, as schematically depicted in Figure 9, though their intensity and temporal evolution may be greatly modified depending upon the nature of current closure path and the electrical conductivity of the regolith (Slavin *et al.*, 1997). When the magnetic flux tubes in the tail reconnect again and high-speed plasma jets are generated toward and away from the planet (see Figure 7), another set of field-aligned currents are generated, termed the "substorm current wedge (SCW)" (McPherron *et al.*, 1973; Hesse and Birn, 1991; Shiokawa *et al.*, 1998). These currents are also shown in Figure 9. The SCW currents connect the

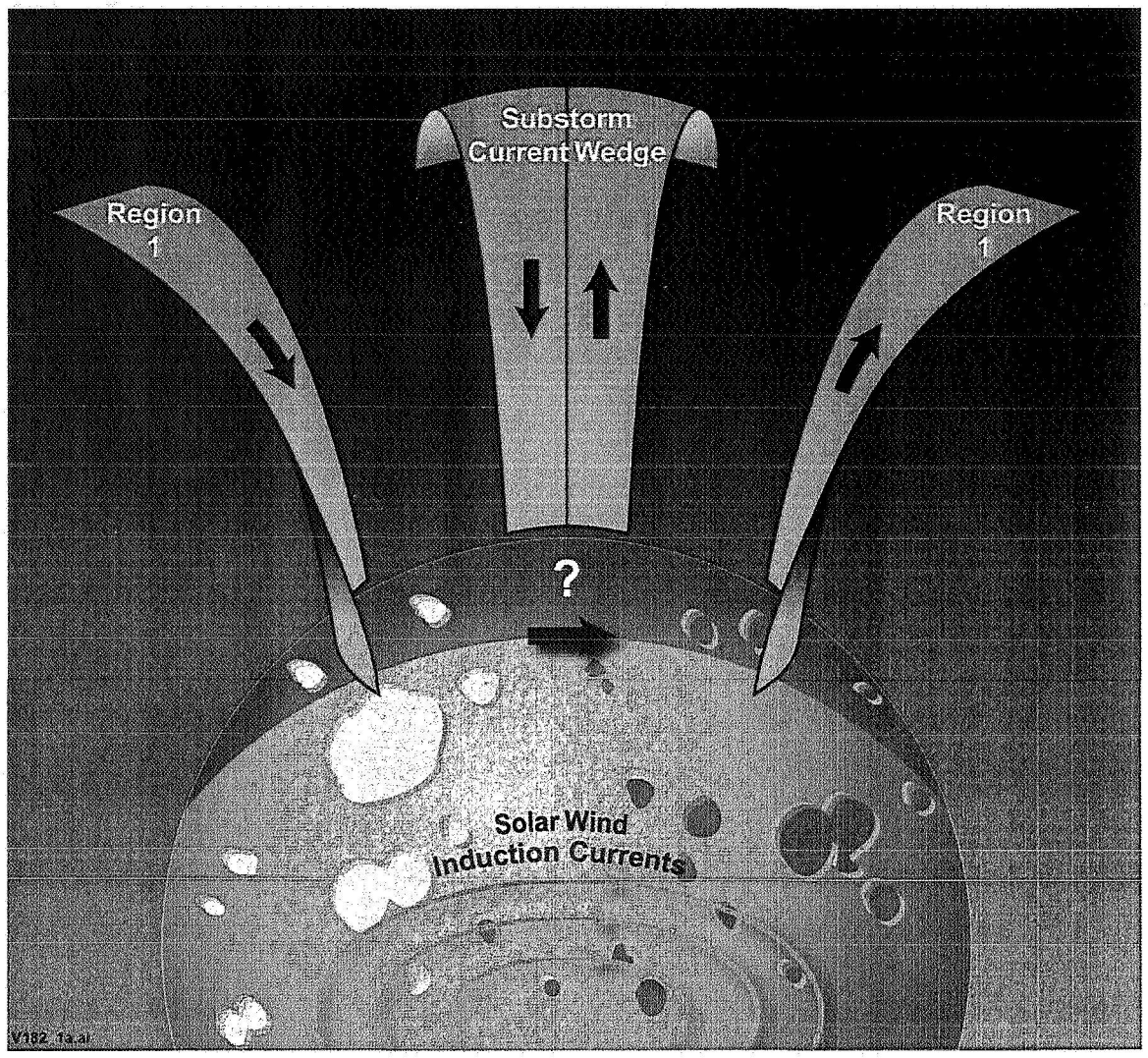


**Figure 9.** Depiction of possible Region 1 and substorm current wedge field-aligned currents at high latitudes. Subsurface solar wind induction currents, flowing in the planetary interior, are shown at lower latitudes.

midnight region of the polar cap to the plasma sheet and transfer to the planet a significant fraction of the total energy being released in the tail (e.g., Fedder and Lyon, 1987). These SCW currents are the most likely source of the field-aligned currents in the Mariner 10 measurements reported by Slavin *et al.* (1997). Numerical simulations by Janhunen and Kallio (2004) and Ip and Kopp (2004) suggest that Region 1 and SCW field-aligned currents will have important consequences for the structure of Mercury's magnetosphere as they do for that of Earth (cf. Fedder and Lyon, 1987). However, in order for these currents to reach a steady-state, they must have a conductive path for closure. As Mercury possesses no such conductive ionosphere, other mechanisms or paths must be found.

A moderately conductive regolith is a likely candidate for FAC closure at Mercury. Hill *et al.* (1976) suggested a conductance value of 0.1 mho, which is not unreasonable based upon the lunar measurements. If this value were indeed appropriate, however, the high rate of joule heating in the regolith would severely limit

the duration of the current flow as the available magnetospheric energy would be quickly dissipated. The analysis of the Mariner 10 magnetic field perturbations by Slavin *et al.* (1997), however, suggest a longer duration FAC flow, and imply a higher conductivity closure path. Janhunen and Kallio (2004) have considered the range of possible surface materials and mineralogy and concluded that a wide range of effective height-integrated conductances are plausible. In the absence of detailed measurements, the electrodynamic coupling between the planet and the magnetosphere cannot be specified.

Cheng *et al.* (1987) showed that sputtering is a possible means to generate the neutral sodium atmosphere of Mercury and a source population for magnetospheric ions. Cheng *et al.* pointed out that the new ions created by photo-ionization, electron impact ionization, and charge exchange are available to be "picked-up" by the convective motion of the magnetospheric flux tubes (Figure 6). In doing so, they would give rise to a "pickup" or "mass loading" conductance (see Kivelson, 2005) that might contribute to the generation and/or closure of FACs at Mercury. Photoelectrons have also been suggested as a source of current carriers (Grard *et al.*, 1999; Grard and Balogh, 2001). However, the pick-up of planetary ions and the photoelectron sheath over Mercury's sunlit surface provide conductances that are only slightly greater than the lunar values. Measurements of surface characteristics, as well as neutral and ion populations near the surface of Mercury, are necessary for a better understanding of magnetosphere-surface coupling.

## 6.4 HOW WILL MESSENGER DETECT AND MAP FIELD-ALIGNED CURRENTS AND DETERMINE THEIR CLOSURE PATH?

The large scale field-aligned currents at Mercury should be readily detected by MESSENGER instrumentation. The signatures of currents at low altitudes in the Earth system are well known (Iijima and Potemra, 1978; Zanetti and Potemra, 1982). The low altitude northern hemisphere portion of the MESSENGER orbit, as depicted in Figures 3a and b, is ideal for detecting field-aligned currents since the magnetic perturbation scales as $r^{-3/2}$ (Rich *et al.*, 1990). Experience at the Earth shows that the infinite-current-sheet assumption enables the accurate inference of field-aligned current density from single spacecraft measurements (Rich *et al.*, 1990; Anderson *et al.*, 1998; 2000). Although this approach breaks down more than a few hours from dawn and dusk and under other circumstances (e.g., northward IMF) when fringing effects dominate the signatures, the magnetic signatures unambiguously indicate the presence of the currents even if one cannot confidently infer the current density distribution from the data (cf. Fung and Hoffman, 1992; Waters *et al.*, 2001; Korth *et al.*, 2005). In addition, particle data provide useful correlative observations of the current carriers, and the FIPS and EPS sensors which measure composition, velocity and density for both ions and electrons will, in principle, give a direct measurement of current. As most current carriers are of relatively low energy, the broad energy range of EPPS will be of particular importance. Finally, GRNS, XRS and other

instruments will provide data about the makeup of the regolith, allowing better estimates of the surface's conductivity.

## 7. Summary

A common paradigm describing the accumulation of knowledge about a planetary body suggests that advances come in four mission phases: "reconnaissance", "exploration," "intensive study," and "understanding". Applied to Mercury, the Mariner 10 mission can be said to have contributed to our understanding by providing a reconnaissance-level characterization. In particular, those measurements showed that Mercury possesses an intrinsic magnetic field that interacts strongly with the solar wind, especially when the IMF is southward, and produces short-duration, intense variations in the tail magnetic field that are well correlated with energetic particle acceleration events.

As described here, the MESSENGER mission will explore Mercury's magnetic field and its magnetosphere for the first time. The mission will determine whether the planet's magnetic field is the result of an on-going convective dynamo, some other type of dynamo, or some distribution of crustal magnetization. MESSENGER will also characterize the structure and dynamics of Mercury's magnetosphere and its response to average and extreme interplanetary conditions. In particular, it will determine whether Earth-like "substorms" occur, how the lack of an ionosphere affects magnetospheric dynamics, and the processes responsible for Mercury's intense energetic particle acceleration events. Moreover, the mission will determine the nature and importance of the coupling between this magnetosphere, the exosphere, and the regolith and, through induction, the planetary interior. The importance of magnetospheric charged particle precipitation for the maintenance and variability of the exosphere will be determined. Conversely, the impact of newly formed heavy ions originating from the effect of solar extreme UV radiation on Mercury's exosphere will also be measured. Finally, the existence of field-aligned currents and the nature of their low-altitude closure will be revealed. The success of MESSENGER in achieving these exploration-level and some intensive study objectives will, in turn, produce a foundation for comprehensive investigations to be carried out by future missions such as BepiColombo (Grard, 2001) that should lead to a detailed understanding of this most intriguing of the magnetospheres in our solar system.

## Acknowledgements

The authors express their great appreciation to all of those who have contributed to the MESSENGER mission. Useful comments and discussion with J. Eastwood are gratefully acknowledged.

## References


Acuna, M. H., *et al.*: 1998, Magnetic field and plasma observations at Mars: Initial results from the Mars Global Surveyor mission, *Science* **279**, 1676-1680.

Acuna, M. H., *et al.*: 1999, Global distribution of crustal magnetization discovered by the Mars Global Surveyor MAG/ER experiment, *Science* **284**, 790-793.

Aharonson, O., Zuber, M. T., and Solomon, S. C.: 2004, Crustal remanence in an internally magnetized non-uniform shell: A possible source for Mercury's magnetic field? *Earth Planet. Sci. Lett.* **218**, 261-268.

Anderson, B. J., *et al.*: 2005, The MESSENGER magnetic fields experiment, *Space Sci. Rev.*, submitted.

Anderson, B. J., Erlandson, R. E., and Zanetti, L. J.: 1992, A statistical study of Pc 1–2 magnetic pulsations in the equatorial magnetosphere: 1. Equatorial occurrence distributions, *J. Geophys. Res.* **97**, 3075–3088.

Anderson, B. J., Gary, J. B., Potemra, T. A., Frahm, R. A., Sharber, J. R., Winningham, J. D.: 1998, UARS observations of Birkeland currents and Joule heating rates for the November 4, 1993 storm, *J. Geophys. Res.* **103**, 26323-26335.

Anderson, B. J., Takahashi, K., and Toth, B. A.: 2000, Sensing Birkeland currents with Iridium engineering magnetometer data, *Geophys. Res. Lett.* **27**, 4045-4048.

Andrews, G. B., *et al.*: 2005, The MESSENGER Energetic Particle and Plasma Spectrometer, *Space Sci. Rev., submitted.*

Angelopoulos, V., *et al.*: 1992, Bursty bulk flows in the inner central plasma sheet, *J. Geophys. Res.* **97**, 4027-4039.

Armstrong, T. P., Krimigis, S. M., and Lanzerotti, L. J.: 1975, A reinterpretation of the reported energetic particle fluxes in the vicinity of Mercury, *J. Geophys. Res.* **80**, 4015-4017.

Baker, D. N., Simpson, J. A., and Eraker, J. H.: 1986, A model of impulsive acceleration and transport of energetic particles in Mercury's magnetosphere, *J. Geophys. Res.* **91**, 8742-8748.

Baker, D. N., Anderson, R. C., Zwickl, R. D., and Slavin, J. A.: 1987, Average plasma and magnetic field variations in the distant magnetotail associated with near-Earth substorm effects, *J. Geophys. Res.*, *92*, 71-81.

Baker, D. N., Pulkkinen, T. I., Angelopoulos, V., Baumjohann, W., and McPherron, R. L.: 1996, Neutral line model of substorms: Past results and present view, *J. Geophys. Res.* **101**, 12975-13010.

Bargatze, L. F., Baker, D. N., McPherron, R. L., and Hones, E. W., Jr.: 1985, Magnetospheric impulse response for many levels of geomagnetic activity, *J. Geophys. Res.* **90**, 6387-6394.

Bida, T. A., Killen, R. M., and Morgan, T. H.: 2000, Discovery of calcium in Mercury's atmosphere, *Nature* **404**, 159-161.

Blomberg, L. G.: 1997, Mercury's magnetosphere, exosphere and surface: Low-frequency field and wave measurements as a diagnostic tool, *Planet. Space Sci.* **45**, 143-148.

Buchner, J., and Zelenyi, L. M.: 1989, Regular and chaotic charged particle motion in magnetotail-like field reversals: 1. Basic theory, *J. Geophys. Res.* **94**, 11821-11842.

Burlaga, L. F.: 2001, Magnetic fields and plasmas in the inner heliosphere: Helios results, *Planet. Space Sci.* **49**, 1619-1627.

Cheng, A. F., Johnson, R. E., Krimigis, S. M., and Lanzerotti, L. J.: 1987, Magnetosphere, exosphere and surface of Mercury, *Icarus* **71**, 430-440.

Christon, S. P.: 1987, A comparison of the Mercury and Earth magnetospheres: Electron measurements and substorm time scales, *Icarus* **71**, 448-471.

Christon, S. P., Feynman, J., and Slavin, J. A.: 1987, Substorm injection fronts: Similar magnetospheric phenomena at Earth and Mercury, *Magnetotail Physics*, A. T. Y. Lui, pp. 393-402, Johns Hopkins University Press, Baltimore, 1987.

Coates, A. J., Johnstone, A. D., and Neubauer, F. M.: 1996, Cometary ion pressure anisotropies at comets Halley and Grigg-Skjellerup, *J. Geophys. Res.* 101, 27573-27584.

Connerney, J. E. P., and Ness, N. F.: 1988, Mercury's magnetic field and interior, in F. Vilas, C. R. Chapman, and M. S. Matthews (eds.), *Mercury,* University of Arizona Press, Tucson, Arizona, pp. 494–513.

Coroniti, F. V., and Kennel, C. F.: 1973, Can the ionosphere regulate magnetospheric convection?, *J. Geophys. Res.* **78**, 2837-2851.

Cowley, S. W. H.: 1980, Plasma populations in a simple open model magnetosphere, *Space Sci. Rev.* **25**, 217-275.

Cowley, S. W. H., et al: 2005, Reconnection in a rotation dominated magnetosphere and its relation to Saturn's auroral dynamics, *J. Geophys. Res.* 110, A02201, doi:10.1029/2004JA010796.

Delcourt, D. C., Moore, T. E., Orsini, S., Millilo, A., Sauvaud, J.-A.: 2002, Centrifugal acceleration of ions near Mercury, *Geophys. Res. Lett.* **29**, doi:10.1029/2001GL013829.

Delcourt, D. C., *et al.*: 2003, A quantitative model of planetary $Na^+$ contribution to Mercury's magnetosphere, *Ann. Geophys.* **21**, 1723-1736.

Domingue, D., *et al.*: 2005, Mercury's atmosphere: A surface-bounded exosphere, *Space Sci. Rev.,submitted.*

Eraker, J. H., and Simpson, J. A.: 1986, Acceleration of charged particles in Mercury's magnetosphere, *J. Geophys. Res.* **91**, 9973-9993.

Fedder, J. A., and Lyon, J. G.: 1987, The solar wind – magnetosphere – ionosphere current – voltage relationship, *Geophys. Res. Lett.* **14**, 880-883.

Fung, S. F., and Hoffman, R. A.: 1992, Finite geometry effects of field-aligned currents, *J. Geophys. Res.* **97**, 8569-8579.

Giampieri, G., and Balogh, A.: 2001, Modeling of magnetic field measurements at Mercury. *Planet. Space Sci.* 49, 1637–1642.

Giampieri, G., and Balogh, A.:, 2002, Mercury's thermoelectric dynamo revisited, *Planet. Space Sci.* **50**, 757–762.

Glassmeier, K. -H.: 1997, The Hermean magnetosphere and its I-M coupling, *Planet. Space Sci.* **45**, 119-125.

Glassmeier, K. -H., Mager, N. P., Klimushkin, D. Y.: 2003, Concerning ULF pulsations in Mercury's magnetosphere, *Geophys. Res. Lett.* **30**, doi:10.1029/2003GL017175.

Gold, R. E., *et al.*: 2001, The MESSENGER mission to Mercury: Scientific payload. *Planet. Space Sci.* **49**, 1467–1479.

Goldstein *et al.*: 2005, *Space Sci. Rev., submitted.*

Goldstein, B. E., Suess, S. T., Walker, R. J.: 1981, Mercury: Magnetospheric processes and the atmospheric supply and loss rates, *J. Geophys. Res.* **86**, 5485-5499.

Gomberoff, L. and H. F. Astudillo, 1998. Electromagnetic ion-beam-plasma instabilities, *Planet. Space Sci.* 46, 1683-1687.

Grard, R., and Balogh, A.: 2001, Return to Mercury: Science and mission objectives, *Planet. Space Sci.* **49**, 1395-1407.

Grard, R., Laakso, H., Pulkkinen, T. I.: 1999, The role of photoemission in the coupling of the Mercury surface and magnetosphere, *Planet. Space Sci.* **47**, 1459-1463.

Grosser, J., Glassmeier, K. -H., and Stadelmann, S.: 2004, Induced magnetic field effects at planet Mercury, *Planet. Space Sci.* **52**, 1251-1260.

Hesse, M., and Birn, J.: 1991, On dipolarization and its relation to the substorm current wedge, *J. Geophys. Res* **96**, 19417-19426.

Hill, T. W.: 1975, Magnetic merging in a collisionless plasma, *J. Geophys. Res.* **80**, 4689-4699.

Hill, T. W., Dessler, A. J., and Wolf, R. A.: 1976, Mercury and Mars: The role of ionospheric conductivity in the acceleration of magnetospheric particles, *Geophys. Res. Lett.* **3**, 429-432.

Hones, E. W., Jr., *et al.*: 1984, Structure of the Magnetotail at 220 $R_e$ and Its Response to Geomagnetic activity, *Geophys. Res. Lett.* **11**, 5-7.

Hoshino, H.: 2005, Electron surfing acceleration in magnetic reconnection, *J. Geophys. Res.* **110**, A102154, doi:10.1029/2005JA011229.

Hood, L. L., and Schubert, G.: 1979, Inhibition of solar wind impingement on Mercury by planetary induction currents, *J. Geophys. Res.* **84**, 2641-2647.

Hunten, D. M., Morgan, T. H., and Schemansky, D. E.: 1988, The Mercury Atmosphere, in F. Vilas, C. R. Chapman, and M. S. Matthews (eds.)*Mercury,* Univ. of Arizona Press, Tucscon, Arizona, pp. 562-612.

Iijima, T., and Potemra, T. A.: 1978, Large-scale characteristics of field-aligned currents associated with substorms, *J. Geophys. Res.* **83**, 599-615.

Ip, W. -H.: 1987, Dynamics of electrons and heavy ions in Mercury's magnetosphere, *Icarus* **71**, 441-447.

Ip, W. -H., and Kopp, A.: 2002, MHD simulation of the solar wind interaction with Mercury, *J. Geophys. Res.* **107**, doi:10.1029/2001JA009171.

Ip, W. -H., and Kopp, A.: 2004, Mercury's Birkeland current system, *Adv. Space. Res.* **33**, 2172-2175.

Jackson, D. J., and Beard, D. B.: 1977, The magnetic field of Mercury. *J. Geophys. Res.* 82, 2828–2836.

Janhunen, P., and Kallio, E.: 2004, Surface conductivity of Mercury provides current closure and may affect magnetospheric symmetry, *Annales Geophys.* 22, 1829-1830.

Kabin, K., *et al.*: 2000, Interaction of Mercury with the solar wind, *Icarus* **84**, 397-406.

Kazama, Y., and Mukai, T.: 2005, Simultaneous appearance of energy-dispersed ion signatures of ionospheric and magnetotail origins in the near-Earth plasma sheet, *J. Geophys Res.* **110**, A07213, doi:10.1029/2004JA010820.

Killen, R. M. and Ip, W. H.: 1999, The surface bounded atmospheres of Mercury and the Moon, *Rev. Geophys. Space Phys.* **37**, 361-406.

Killen, R. M., *et al.*: 2001, Evidence for space weather at Mercury, *J. Geophys. Res.* **106**, 20509-20525.

Killen, R. M., Sarantos, M., Potter, A. E., Reiff, P. H.: 2004, Source rates and ion recycling rates for Na and K in Mercury's atmosphere, *Icarus* **171**, 1-19.

Kivelson, M. G.: 2005, The current systems of the Jovian magnetosphere and ionosphere and predictions for Saturn, *Space Sci. Rev.* **116**, 299-318.

Koehn, P. L.: 2002, The development and testing of the Fast Imaging Plasma Spectrometer and its application in the plasma environment of Mercury, PhD Thesis, University of Michigan, Ann Arbor, Michigan.

Korth, H., *et al.*: 2004, Determination of the properties of Mercury's magnetic Field by the MESSENGER mission, *Planet. Space Sci.* **54**, 733-746.

Korth, J., Anderson, B. J., Frey, and Waters, C. L.:2005, High-latitude electromagnetic and particle energy flux during an event with sustained strongly northward IMF, *Annales Geophys.* **23**, 1295-1310.

Krimigis, S. M. and Sarris, E. T.: 1979, Energetic particle bursts in the Earth's magnetotail, *Dynamics of the Magnetosphere,* ed. by S. -I. Akasofu (ed.), D. Reidel, Dordrecht, Holland, 599-630.

Lammer, H., and Bauer, S. J.: 1997, Mercury's exosphere: Origin of surface sputtering and implications, *Planet. Space Sci.* **45**, 73-79.

Lammer, H., et al.: 2003, The variability of Mercury's by particle and radiation induced surface release processes, *Icarus* **166,** 238-247.

Leblanc, F., Luhmann, J. G., Johnson, R. E., and Lui, M.: 2003, Solar energetic particle event at Mercury, *Planet. Space Sci.* **51**, 339-352.

Luhmann, J. G., Russell, C. T., and Tsyganenko, N. A.: 1998, Disturbances in Mercury's magnetosphere: Are the Mariner 10 "substorms" simply driven? *J. Geophys. Res.***103**, 9113–9119.

Lukyanov, A. V., Barabash, S., Lundin, R., Brandt, and P. C:son: 2001, Energetic neutral atom imaging of Mercury's magnetosphere: 2. Distribution of energetic charged particles in a compact magnetosphere, *Planet. Space Sci.* **49**, 1677-1684.

Massetti, S., et al.: 2003, Mapping of the cusp plasma precipitation on the surface of Mercury, *Icarus* **166**, 229-237.

Mauk, B. H.: 1986, Quantitative modeling of the "convective surge" mechanism of ion acceleration, *J. Geophys. Res.* **91**, 13423-13431.

McClintock, W., *et al.*: 2005, *Space Sci. Rev., submitted.*

McPherron, R. L., Russell, C. T., Aubry, M. P.: 1973, Satellite studies of magnetospheric substorms on August 15, 1968, 9. Phenomenological model for substorms, *J. Geophys.Res.* **78**, 3131-3149.

Mitchell, D. G., *et al.*: 2005, Energetic ion acceleration in Saturn's magnetotail: Substorms at Saturn?, *Geophys. Res. Lett.* **32,** L20S01, doi:10.1029/2005GL022647.

Milillo, A., *et al.*: 2005, Surface-exosphere-magnetosphere system of Mercury, *Space Sci. Rev.* **117**, 397-443.

Mukai, T., Ogasawara, K., and Saito, Y.: 2004, An empirical model of the plasma environment around Mercury, *Adv. Space Res.* **33**, 2166-2171.

Ness, N. F., Behannon, K. W., Lepping, R. P., and Whang, Y. C., Schatten, K. H.: 1974, Magnetic field observations near Mercury: Preliminary results from Mariner 10, *Science* **185**, 151–160.

Ness, N. F., Behannon, K. W., and Lepping, R. P.: 1975. The magnetic field of Mercury, *J. Geophys. Res.* **80**, 2708–2716.

Ness, N. F., Behannon, K. W., Lepping, R. P., and Whang, Y. C.: 1976, Observations of Mercury's magnetic field, *Icarus* **28**, 479–488.

Ogilvie, K. W., *et al.:* 1974, Observations at Mercury encounter by the plasma science instrument on Mariner 10, *Science* **185**, 145-150.

Ogilvie, K. W., Scudder, J. D., Vasyliunas, V. M., Hartle, R. E., and Siscoe, G. L.: 1977, Observations at the planet Mercury by the plasma electron instrument: Mariner 10, *J.Geophys. Res.* **82**, 1807-1824.

Potter, A. E., and Morgan, T. H.: 1985, Discovery of sodium in the atmosphere of Mercury, *Science* **229**, 651-653.

Potter, A. E., and Morgan, T. H., 1986, Potassium in the atmosphere of Mercury, *Icarus* **67**, 336-340.

Potter, A. E., Killen, R. M., and Morgan, T. H.: 1999, Rapid changes in the atmosphere of Mercury, *Planet. Space Sci.* **47**, 1441-1448.

Rich, F. J., Hardy, D. A., Redus, R. H., and Gussenhoven, M. S.: 1990, Northward IMF and patterns of high-latitude precipitation and field-aligned currents: The February 1986 storm, *J. Geophys. Res.* **95**, 7893-7913.

Richardson, I. G., Owen, C. J., and Slavin, J. A.: 1996, Energetic (>0.2 MeV) electron bursts in the deep geomagnetic tail observed by the Goddard Space Flight Center Experiment on ISEE-3: Association with geomagnetic substorms, *J. Geophys. Res.* **101**, 2723-2740.

Runcorn, S. K.: 1975a,. An ancient lunar magnetic dipole field, *Nature* **253**, 701–703.

Runcorn, S. K.: 1975b, On the interpretation of lunar magnetism, *Phys. Earth Planet. Inter.* **10**, 327–335.

Russell, C. T.: 1977, On the relative locations of the bow shocks of the terrestrial planets, *Geophys. Res. Lett.* **4**, 387-390.

Russell, C. T., and Walker, R. J.: 1985, Flux transfer events at Mercury, *J. Geophys. Res.* **90**, 11067-11074.

Russell, C. T., Baker, D. N, and Slavin, J. A.: 1988, The magnetosphere of Mercury, in F. Vilas, C. R. Chapman, and M. S. Matthews (eds.)*Mercury,* University of Arizona Press, Tucscon, Arizona, pp. 514-561.

Russell, C. T.: 1989, ULF waves in the Mercury magnetosphere, *Geophys. Res. Lett*, **16**, 1253-1256.

Santo, A. G., *et al.*: 2001, The MESSENGER mission to Mercury: Spacecraft and mission design, *Planet. Space Sci.* **49**, 1481–1500.

Sarantos, M.: 2000, An open magnetosphere model for Mercury, M.S. thesis, Rice University, Houston, Texas.

Sarantos, M., Reiff, P. H., Hill, T. W., Killen, R. M., and Urquhart, A. L.: 2001, A $B_x$-interconnected magnetosphere model for Mercury, *Planet. Space Sci.* **49**, 1629-1635.

Sarris, E. T., and Axford, W. I.: 1979, Energetic protons near the plasma sheet boundary, *Nature* **77**, 460-462.

Sasaki, S., and Kurahashi, E.: 2004, Space weathering on Mercury, *Adv. Space. Res.* **33**, 2152-2155.

Sauvaud, J. -A., *et al.*: 1999, Sporadic plasma sheet ion injections into the high-latitude auroral bulge: satellite observations, *J. Geophys. Res.* **104**, 28565-28586.

Schlemm *et al.*: 2005, *Space Sci. Rev., submitted.*

Scholer, M., Gloecker, G., Klecker, B., Ipavich, F. M., Hovestadt, D., and Smith, E. J.: 1984, Fast moving plasma structures in the distant magnetotail, *J. Geophys. Res.* 89, 6717-6727.

Shiokawa, K., *et al.:* 1998, High-speed ion flow, substorm current wedge formation and multiple Pi2 pulsations, *J. Geophys. Res.* **103**, 4491-4507.

Sibeck, D. G., Lopez, R. E., and Roelof, E. C.: 1991, Solar wind control of magnetopause shape, location and motion, *J. Geophys. Res.* **96**, 5489-5495.

Simpson, J. A., Eraker, J. H., Lamport, J. E., and Walpole, P. H.: 1974, Electrons and protons accelerated in Mercury's Magnetosphere, *Science* **185**, 160-166.

Siscoe, G. L., and Christopher, L.: 1975, Variations in the solar wind stand-off distance at Mercury, *Geophys. Res. Lett.,* **2**, 158-160.

Siscoe, G. L., Ness, N. F., and Yeates, C.M.: 1975, Substorms on Mercury?, *J. Geophys. Res.* **80**, 4359-4363.

Slavin, J. A.: 2004, Mercury's magnetosphere, *Adv. Space Res.* **33**/11, 1587-1872.

Slavin, J. A., and Holzer, R. E.: 1979a, The effect of erosion on the solar wind stand-off distance at Mercury, *J. Geophys. Res.* **84**, 2076-2082.

Slavin, J. A., and Holzer, R. E.: 1979b, On the determination of the Hermean magnetic moment: A critical review, *Phys. Earth Planet. Interiors* **20**, 231-236.

Slavin, J. A., and Holzer, R. E.: 1981, Solar wind flow about the terrestrial planets, 1. Modeling bow shock position and shape, *J. Geophys. Res.* **86**, 11401-11418.

Slavin, J. A., Owen, C.J., Connerney, J.E.P., and Christon, S.P.: 1997, Mariner 10 observations of field-aligned currents at Mercury, *Planet. Space Sci.* **45**, 133-141.

Slavin, J. A., *et al.:* 2002, Simultaneous observations of earthward flow bursts and plasmoid ejection during magnetospheric substorms, *J. Geophys. Res.* **107**, doi:10.1029/2000JA003501.

Solomon, S. C.: 1976, Some aspects of core formation in Mercury, *Icarus*, **28**, 509–521.

Solomon, S. C., et al.: 2001, The MESSENGER mission to Mercury: Scientific objectives and implementation, *Planet. Space Sci.* **49**, 1445-1465.

Southwood, D. J., and M. G. Kivelson: 1981, Charged particle behavior in low-frequency geomagnetic pulsations 1. Transverse waves, *J. Geophys. Res.* **86**, 5643–5655.

Srnka, L. J.: 1976, Magnetic dipole moment of a spherical shell with TRM acquired in a field of internal origin. *Phys. Earth Planet. Inter.* **11**, 184–190.

Stephenson, A.: 1976, Crustal remanence and the magnetic moment of Mercury, *Earth Planet. Sci. Lett.* **28**, 454–458.

Stevenson, D. J.: 1983. Planetary magnetic fields, *Rep. Prog. Phys.* **46**, 555–620.

Stevenson, D. J., 1987. Mercury's magnetic field: A thermoelectric dynamo? *Earth Planet. Sci. Lett.* **82**, 114–120.

Stevenson, D. J., Spohn, T., and Schubert, G.: 1983. Magnetism and thermal evolution of the terrestrial planets. *Icarus* **54**, 466–489.

Suess, S. T., and Goldstein, B. E.: 1979, Compression of the Hermaean magnetosphere by the solar wind, *J. Geophys. Res.* **84**, 3306-3312.

Teresawa, T., *et al.*: 1997, Solar wind control of the plasma sheet, *Geophys. Res. Lett.* **24**, 935-938``.

Tanskanen, E. I., *et al.*: 2005, Response of the magnetotail to prolonged southward $B_z$ intervals: Loading, unloading, and continuous dissipation, *J. Geophys. Res.* ***110***, A03216, doi:10.1029/2004JA010561.

Waters, C. L., Anderson, B. J., Liou, K.: 2001, Estimations of global field-aligned currents using Iridium magnetometer data, *Geophys. Res. Lett.* **28**, 2165-2168.

Whang, Y. C.: 1977, Magnetospheric magnetic field of Mercury. *J. Geophys. Res.* **82**, 1024–1030.

Zanetti, L. J., and Potemra, T. A.: 1982, Correlated Birkeland current signatures from the Triad and MAGSAT magnetic field data, *Geophys. Res. Lett.* **9**, 349-352.

Zurbuchen, T. H., Koehn, P., Fisk, Gombosi, T., Gloeckler, G., and Kabin, K.: 2004, On the space environment of Mercury, *Adv. Space Res.* **33**, 1884-1889.